C.P. No. 1108

C.P. No. 1108

MINISTRY OF TECHNOLOGY

AERONAUTICAL RESEARCH COUNCIL

CURRENT PAPERS

Low-Speed Wind-Tunnel Tests on an Unswept Wing-Fuselage Model of Aspect Ratio 9·8, with Tangential Blowing over Trailing-Edge Flaps and Ailerons, including the Effect of Slipstream

by

J. A. Lawford

Aerodynamics Dept., R.A.E., Farnborough

LONDON: HER MAJESTY'S STATIONERY OFFICE

1970

PRICE *16s 0d* [*80p*] NET

U.D.C. 533.693.2 : 533.6.072 : 533.694.511 : 533.695.8 :
533.6.071 : 533.6.011.32/34

C.P. No. 1108*
May 1968

LOW-SPEED WIND-TUNNEL TESTS ON AN UNSWEPT WING-FUSELAGE MODEL OF ASPECT RATIO 9·8, WITH TANGENTIAL BLOWING OVER TRAILING-EDGE FLAPS AND AILERONS, INCLUDING THE EFFECT OF SLIPSTREAM

by

J. A. Lawford
Aerodynamics Department, R.A.E., Farnborough

SUMMARY

Tests have been made on an unswept, high-wing wing-fuselage model of aspect ratio 9·8, with boundary layer control by blowing at the shroud of trailing-edge flaps and ailerons. Propeller slipstream was represented during some of the tests.

Critical blowing momentum coefficients were determined; these ranged from 0·015 to 0·05 at flap angles of 30° and 60° respectively. With slipstream, a critical coefficient defined in terms of slipstream velocity at the propeller disc was substantially independent of thrust coefficient.

Increments of lift coefficient, without slipstream, due to a blowing momentum coefficient of 0·1, were 0·65 and 1·82 respectively at flap angles of 0° and 60°.

*Replaces R.A.E. Technical Report 68111 - A.R.C. 30636.

CONTENTS

1 INTRODUCTION

This Report gives results of low-speed wind-tunnel tests on an unswept wing-fuselage model of aspect ratio 9·8, to find the effect of blowing over trailing-edge flaps and ailerons on the aerodynamic characteristics. The determination of the blowing quantities required to obtain attached flow for a range of flap angles, including the effect of slipstream, was an important part of the experiment.

The model used for the tests was representative of the wing-fuselage arrangement of a proposed high-wing transport aircraft. The flaps and ailerons extended from just outboard of the fuselage to the wing tip, and the blowing slot, which extended over the entire flap/aileron span, was tapered in depth in proportion to the chord of the slightly tapered wing, with the intention of achieving uniformity of sectional blowing momentum coefficient over the span. Two separate series of tests were made. During the first, defects in the quality of the blowing slot and some basic disadvantages of the model became apparent; as a result there was considerable variation of the value of mean blowing momentum required to obtain attached flow at various spanwise positions; this may have been due to local variation of critical momentum required, or of local momentum achieved for a given mean value or, more probably, a combination of both. The blowing slot was improved prior to the second series of tests but while this gave some local improvements, spanwise variation remained, and while there was some increase of lift at constant incidence, maxima were not improved. The effects of propeller slipstream were investigated during the first series, but this was not repeated during the second series.

These tests, which were made in the 24ft wind tunnel at the R.A.E. during 1962 and 1963, were the first in the Low Speed Tunnels Division in which it was attempted to pass air into a model through the centre of a strain gauge balance. The tests showed the method to be successful apart from some minor defects in detail. The arrangement of the rig and its calibration have been fully described by Eyre[1].

A blowing momentum coefficient C'_μ defined in terms of the blown area of the wing is used in this Report. If constancy of sectional momentum coefficient over the blown area had been achieved exactly, C'_μ would equal this sectional value, and in the presence of some local variation, it is representative of mean conditions over the blown area.

2 MODEL DETAILS

The main details of the model are given in Table 1, and the general arrangement of the model and details of the blowing slot in Fig.1. A photograph and drawing of the arrangement in the 24ft wind tunnel are given in Figs.2 and 3 respectively. For the tests without slipstream the wing was "clean", without nacelles. The model had no fin or tailplane.

The control* upper surfaces forward of the hinge were curved (Fig.1) with centres at the control hinge, and the blowing slot was aligned to blow tangentially on the curved surface. Cover plates extended rearwards from the lower surface to maintain the wing contour: the lower surface of the ailerons forward of the hinge was chamfered so that it remained within the cover plate at upward aileron deflection.

The modifications made between the two series of tests consisted of stiffening the blowing slot upper lip to prevent local distortion, removal of small internal blocks at the dihedral kinks, and fitting internal vanes to improve air distribution at the inboard end of the blowing slot. More complete details are given in Ref.1.

3 DETAILS OF TESTS

Most of the tests were made at a wind speed of 100 ft/s (giving a Reynolds number based on aerodynamic mean chord, $\bar{c}$, of $0{\cdot}9 \times 10^6$). Transition was fixed on the fuselage by a wire at approximately one maximum radius aft of the nose and was free on the wing except where otherwise stated. Some comparisons at 140 ft/s showed little change in the critical value C'_{μ_a} of the blowing momentum coefficient. Some of the tests with slipstream were made at speeds below 100 ft/s, in order to obtain the required values of thrust and momentum coefficients. Sealing the gaps between wing and controls was found to have little effect on forces or critical blowing quantities, and these were left unsealed for the main tests. The gaps between the inboard and outboard flaps were sealed for all the tests; those between outboard flaps and ailerons were sealed when these controls were at equal angles. The following tests were made during the two series. (The range of configurations and blowing quantities for which force and moment measurements were taken is summarised in Table 2.)

---

* The model being tail-less, the term "control" is used in this Report to refer to the flaps and ailerons together.

3.1 "Clean" wing, without nacelles

(i) Assessment of critical blowing quantities by means of trailing-edge pressures, tuft observations, and balance measurements.

(ii) Six-component balance measurements, over a range of incidence from -5·5° to the stall, for various combinations of flap and aileron angle, mainly with symmetrical aileron deflection but including some asymmetric conditions. Unyawed.

(iii) Six-component balance measurements over a range of yaw angle from -20° to +20°, for various symmetrical deflections of flap and aileron. Incidences 0°, 3°, 6°, 9°. C'_μ = 0 to 0·1.

(iv) Measurements of aileron effectiveness.

(v) Measurements of hinge moments on flaps and ailerons, at blowing coefficients from 0 to 0·1, and incidences from -5·5° to 15°, for various symmetrical flap and aileron deflections.

(vi) Assessment of stalling behaviour by tuft observations, for various control settings and blowing momentum coefficients.

(vii) Measurement of the effect of a spanwise wire on the wing, on forces, moments, and boundary layer thickness.

3.2 Wing with nacelles and propellers

(i) Assessment of critical blowing quantities by trailing-edge pressures, for various control settings and thrust coefficients.

(ii) Six-component balance measurements, over a range of incidence from -5·5° to the stall, for various symmetrical combinations of control angle, without yaw. T_c range 0 to 4·1. C'_μ range up to 0·25.

4 ASSESSMENT OF BLOWING REQUIREMENTS

4.1 Criteria for the determination of critical blowing quantities

Williams and Butler[2] give three possible criteria for the assessment of the critical sectional blowing coefficient C'_{μ_a}. These are:-

(a) That giving attached flow as indicated by tufts or pressure recovery at or near the trailing-edge.

(b) That giving the estimated theoretical lift increment for the flap corresponding to inviscid flow.

(c) That corresponding to rapid reduction in the slope of the C_L vs. C'_μ curve.

Of these (b) and (c) depend upon uniform behaviour over the span, which was not obtained during the present tests. In these circumstances (b) gives an overestimate of the critical coefficient; the sectional C_L vs. C'_μ curve is steeper below the critical condition than it is above, so that a comparatively high lift loss at a small sub-critical region must be balanced by substantial over-blowing elsewhere, giving a mean value above that which would obtain in uniform conditions. With criterion (c) the gradual flattening of the mean C_L vs. C'_μ curve resulting from spanwise spread of attached flow as C'_μ is increased gives a very ill-defined assessment of a critical value. It therefore appeared best in these tests to rely mainly on criterion (a), and, since heavy tufting may of itself cause flow separation at near-critical conditions, pressure recovery at or near the trailing-edge has been used primarily in determining C'_{μ_a}.

For the first series of tests pressure tappings were fitted in the flaps and ailerons at 95% chord on the upper surface, and these gave a good indication of pressure recovery close to the trailing-edge: prior to the second series it was decided that an improved indication of trailing-edge conditions, with a better defined slope change and reduced dependence on incidence, should be obtained from tappings in the trailing-edge, pointing downstream, and these were fitted (using more trailing-edge tappings than had been used originally at 95% chord). In fact these trailing-edge tappings gave less distinct changes of slope in the C_p vs. C'_μ curve than the ones at 95% chord.

The critical value C'_{μ_a} indicated by a curve of C_p vs. C'_μ has been taken as the value of C'_μ corresponding to a sharp reduction in the slope of the curve, usually at a small positive value of C_p. Fig.4 shows a comparison of tuft indication of local attachment and C_p vs. C'_μ curves at a number of spanwise stations. Correlation is not very good - possibly in part because of the spanwise separation of tapping and tuft necessary to avoid interference, but the above method of assessing C'_{μ_a} is, broadly

speaking, supported by the results. (The curve at $y = 0{\cdot}13\ b/2$ differs in basic form from the others and gives no guide to attachment.)

In order to obtain consistent estimates of critical blowing coefficient the value of C'_{μ_a} has been taken in each case from the same region of the starboard wing; this was a region giving early attachment, since delayed attachment is probably due mainly to local defects, and the starboard wing was chosen because in general it gave earlier attachment and more consistent behaviour than the port. (Figs.13 and 15 of Ref.1 show much less local variation of slot total head loss on the starboard wing than on the port. In the absence of a local mass flow measurement the corresponding variation of momentum coefficient cannot be assessed, but it is likely that this also is more uniform on the starboard wing.)

4.2 Critical blowing quantities without slipstream

Figs.5 to 7 show curves of C_p vs. C'_μ for the starboard wing at $\alpha = 0°$ from the first series of tests, C_p being taken at 95% chord on the upper surface, with control angles equal over the span. At angles of 45° and 60° the flow on the entire inboard flap, and on the outboard flap adjacent to the dihedral kink, does not appear to attach on the surface at all within the range of test blowing quantities. Similar curves from the second series (where most C_p values were taken at the trailing edge) are given in Figs.8 to 10. Apart from the inner end of the inboard flap, curves characteristic of attached flow were obtained within the test range of C'_μ at all points, and tuft observations adjacent to the inboard point showed that attachment occurred here also, in spite of the unusual shape of the C_p vs. C'_μ curve (Fig.4). But the lack of uniformity between spanwise stations on the wing was still considerable. The following table gives values of C'_{μ_a} estimated from these curves, and from similar ones at higher incidence.

	First series			Second series	
$\delta_{F,A}$	$\alpha = 0°$	6°	10°	0°	6°
30°	0·01	0·015		0·015	0·02
45°	0·025	0·03	0·03	0·03	0·04
60°	0·05	0·055		0·05	0·055

Values from the second series are slightly greater than from the first. The values of C'_μ are a mean for the whole wing, derived from

total mass flow and mean total head in the slot. The non-uniformity of blowing slot width which existed during the first series would cause greater local disparity from the mean value than occurred on the second, so that true local values of C'_μ at the "good" regions used in assessing C'_{μ_a} were probably somewhat higher than the mean value.

The following are estimates of C'_{μ_a} from criteria (b) and (c).

	(b)				(c)			
	1st series		2nd series		1st series		2nd series	
$\delta_{F,A}$	$\alpha = 0°$	6°	0°	6°	0°	6°	0°	6°
30°	0·022	0·026	0·020	0·027	0·015	0·02	0·015	0·025
45°	0·042	0·052	0·038	0·046	0·03	0·04	0·035	0·04
60°	0·068	0·078	0·066	0·075	0·055	0·065	0·065	(poorly defined)

As expected, these values are higher than those for criterion (a) - very substantially so for (b). Fig.15 shows curves of C_L against α and C'_μ, and the gradual nature of the slope change of the C_L vs. C'_μ curve, and the consequently poor definition of a critical value of C'_μ using criterion (c) is apparent, particularly at the higher control angles.

4.3 Critical blowing quantities with slipstream

For the estimation of critical blowing quantities within a slipstream which covered only part of the span, tufts or pressures near the trailing-edge were the only methods which could be used, and for the present tests only results from stations lying well within the slipstream and giving good flow on the clean wing were useful. In practice this limited the assessment of C'_{μ_a} to one spanwise station on the starboard wing, at which estimates could be based on pressures at 95% chord. (This station is indicated on Fig.1). In Fig.11, C_p at this position is plotted against C'_μ, for each of the three control angle settings and for a range of propeller thrust coefficient T_c, at $\alpha = 0°$. Values of C'_{μ_a}, estimated from the slope change of the curves, are clearly defined and are tabulated below. The table also shows the value of $C'_{\mu_a}/(1 + a)^2$, that is, the value of the critical blowing coefficient based on the slipstream velocity at the propeller disc, derived from simple momentum theory. $\left(a = \frac{1}{2}\left\{\left(1 + \frac{8}{\pi} T_c\right)^{\frac{1}{2}} - 1\right\}\right)$

T_c	$\delta_{F,A} = 30°$		$\delta_{F,A} = 45°$		$\delta_{F,A} = 60°$	
	C'_{μ_a}	$\frac{C'_{\mu_a}}{(1+a)^2}$	C'_{μ_a}	$\frac{C'_{\mu_a}}{(1+a)^2}$	C'_{μ_a}	$\frac{C'_{\mu_a}}{(1+a)^2}$
0	0·014	0·014	0·028	0·028	0·048	0·048
0·4	0·018	0·012	0·034	0·023	0·073	0·050
0·8	0·025	0·013	0·044	0·023	0·088	0·047
1·4	0·033	0·013			0·119	0·048
1·8	0·036	0·013	0·069	0·024	0·140	0·049
2·6					0·168	0·048
4·1					0·200	0·042

As one would expect, the value of C'_{μ_a} increases with slipstream velocity; the critical coefficient based on the velocity at the disc is however substantially constant and in good agreement with values for the clean wing . This is possibly fortuitous and may not be generally the case. Calculation using the theory of Smelt and Davies[3] shows that, for an unobstructed slipstream, the velocity developed at the quarter chord point on this wing is $V_o(1 + 1.85a)$. Increased turbulence in the slipstream may however reduce the critical blowing coefficient, that determined in terms of local velocity at the wing, compared with that for the clean wing without slipstream.

Critical blowing coefficients for both the "clean" wing and the wing with slipstream are plotted against flap angle in Figs.12a and 12b.

4.4 The effect of model configuration and blowing slot defects on local values of critical blowing quantities

The wide variation across the span of the mean value of C'_μ required to give attachment must be due to imperfections of the blowing slot, so that the local value of C'_μ is lower than the mean, or to details of the model configuration which causes a locally high critical value. In particular, delayed attachment in the dihedral kink during the first series of tests was thought to be due to a local blockage of the slot, present for constructional reasons, which extended over about 0·4 in of the span at that point; that at the inboard end of the flap near the wing root appeared attributable to interference effects between the fuselage and the flap. A more detailed investigation of these features was made.

Results of the corresponding position on the port wing and on the inboard flap on the starboard wing, although less representative of conditions at "good" regions of the wing, are consistent with a correlation based on $C'_\mu/(1 + a)^2$.

4.4.1 Slot blockage

During the first series of tests, blockages of 1/8, 1/4, 1/2 and 1 in. were inserted in turn into the blowing slot forward of the mid-point of the starboard outer flap. Tufts on the flap were observed and balance measurements taken at zero incidence over a range of blowing conditions. The tufts indicated that for blockage of 1/4 in. or less the flow remained attached at blowing rates above the critical, but for blockages of 1/2 and 1 in. a region of separated flow on the flap widened spanwise downstream of the blockage at an angle of approximately 30° to the flap chord line, at all supercritical values of blowing coefficient. Fig.13 shows appreciable reduction of lift coefficient due to this blockage in the cases where it causes flow separation.

4.4.2 Wing root conditions

Trailing-edge pressure at $y = 0{\cdot}13\ b/2$ (the inboard end of the flap being at $0{\cdot}11\ b/2$) are shown in Fig.14 for $\alpha = 0°$ and control angles all 60°. The C_p vs. C'_μ curve is very different in form from those elsewhere on the wing, with no pressure recovery with increase of C'_μ above 0·04. A number of modifications were made at the wing root to investigate this. The first consisted of continuing the flap inboard to the fuselage. This altered the curve, making it differ still further from the usual form, with reduced trailing-edge pressure at all values of C'_μ. Further modification by building up a fairing on the fuselage to form a "slab" side, eliminating the acute angle between the upper fuselage and the lower wing surface, again caused a reduction in trailing-edge pressure at values of C'_μ above 0·03.

A large fence was then fitted at $y = 0{\cdot}19\ b/2$ on the starboard wing, extending from 1·5 in. forward of the leading-edge to the trailing-edge of the lowered flap. This fence was therefore in the same position relative to the trailing-edge pressure station at $y = 0{\cdot}205\ b/2$ as the fuselage side was to the station at $y = 0{\cdot}13\ b/2$. The C_p vs. C'_μ curve for $y = 0{\cdot}205\ b/2$, which had been of normal form, then took a form similar to that found at $y = 0{\cdot}13\ b/2$ (Fig.14). The behaviour near the inboard end of the flap appears therefore to be a fuselage proximity effect, possibly due to the fuselage boundary layer.

5 TUFT STUDIES OF THE STALL PATTERN

Tufts on the wing upper surface at 0·2c and 0·5c were used to examine the form of the stall as incidence was increased at constant C'_μ. At $C'_\mu = 0$

the stall originated at the trailing-edge at all control angles. With increasing blowing momentum the stall pattern changed from trailing-edge to leading-edge separation, the change occurring initially at the wing tip, and at increasing values of C'_μ with increasing control angle, as follows:-

$\delta_{F,A}$	C'_μ for change from T.E. to L.E. stall
0°	0·02
30°	0·02
45°	0·04
60°	0·06

6 FORCE AND MOMENT MEASUREMENTS

6.1 Tests made

Table 2 shows the configurations for which force and moment measurements were made. Results plotted in this report are confined mainly to those obtained with equal flap and aileron settings. Results for non-equal settings are available on application to the Librarian, Aerodynamics Department, R.A.E.

6.2 Tests on the "clean" wing, without nacelle

Lift coefficient is shown plotted in "carpet" form against α and C'_μ in Fig.15; values of $C_{L\ max}$ and of C_L at α_o (the incidence for zero lift at $\delta_F = \delta_A = 0°$, $C'_\mu = 0$) are plotted against δ_A and C'_μ in Figs.16 and 17 respectively (non-equal flap and aileron settings being included). In Fig.18 are shown curves of C_D against C_L^2 and C_m against C_L.

Fig.16 shows increments in $C_{L\ max}$ due to a blowing momentum coefficient of 0·10 ranging from 0·65 at flap and aileron angles of zero to 1·82 at a setting of 60°. Because of the associated negative change in pitching moment (Fig.18), increments in maximum $C_{L_{trimmed}}$ would probably be somewhat less - perhaps 0·6 and 1·65 respectively in the above cases.

Measurements of sideforce, yawing moment and rolling moment coefficients for the yawed model have been centralised and are plotted against angle of side-slip in Fig.19.

6.3 Tests with slipstream

Lift coefficient with slipstream is plotted against incidence in Fig.20. Fig.21 shows lift coefficient plotted against propeller thrust

coefficient, for an incidence of -2° at flap and aileron settings of 30° and 60°. Also shown are calculated values for the variation of C_L with T_c derived using the method of Smelt and Davies[3], the calculated increments being added to the lift measured at $T_c = 0$. At $C'_\mu = 0$ the measured lift increment exceeds the estimate; in this case the flow over the flap is separated both with and without slipstream, but increased turbulent mixing in the slipstream probably gives some improvement in the flow. At $C'_\mu = 0{\cdot}10$ agreement between measurement and calculation is fairly good; in this case the blowing momentum is sufficient to give attached flow except at the higher T_c with 60° control setting, where the measured result does fall below the estimate. At $C'_\mu = 0{\cdot}156$ (where there was no measurement of lift at $T_c = 0$, and this has been interpolated from other results) agreement is less good, although the blowing momentum is sufficient to maintain attached flow at a thrust coefficient of 1·8.

6.4 Aileron effectiveness

In Fig.22 rolling moment coefficient is plotted against aileron angle. (The curves shown are for variation of starboard aileron angle only, with port aileron at 0°. Some points are shown for a port aileron deflection of -28°). The effect of flap and aileron blowing in maintaining control power by preventing separation of flow over the control is clearly demonstrated; the effect is substantially reduced when the entire wing is stalled at high incidence and flap angle.

7 HINGE MOMENT MEASUREMENTS

Hinge moments on the flaps and ailerons were measured by strain gauges, and hinge moment coefficients are plotted against control angle and blowing coefficient in Figs.23 to 25.

8 NON-LINEAR EFFECTS AT LOW INCIDENCE

Non-linear variation of lift and pitching moment coefficients with incidence was observed at low incidence with flap angles of 45° and 60°; this is apparent in Figs.15c and 15d, and 18c and 18d, particularly at a C'_μ of 0·04. Only a brief investigation of this was possible; it was found that sealing of inter-control and wing-control gaps had no effect. A 28 SWG wire attached to the wing leading-edge over the whole span to ensure forward transition on the wing partially straightened the $C_L - \alpha$ curve, and moving

the wire to 0·05 c on the upper surface gave an almost linear $C_L - \alpha$ variation, by reducing C_L at the lower incidences. Comparative curves are given in Fig.26. A corresponding straightening of the $C_m - C_L$ curve is shown in Fig.18d.

Comparative measurements of total head in the boundary layer were made at three upper surface positions without and with a wire at 0·05 c on the upper surface, and these are shown in Fig.27. The wire causes an increase in boundary layer thickness, of the order 0·005 c at all three positions. Increase of incidence also causes boundary layer thickening, but the effect of increasing blowing momentum appears rather to be one of increasing total head loss within the boundary layer, because of increased velocity, with little increase in layer thickness.

It appears probable that the non-linearity of the $C_L - \alpha$ curve at $C'_\mu = 0{\cdot}04$ with no wire is due to thickening of the boundary layer with increasing incidence causing loss of lift at a blowing momentum close to the critical value, when the main flow is sensitive to variation of boundary layer thickness. Thickening of the boundary layer by a wire produces a similar effect at lower incidence and so straightens the curve. The partial straightening of the curve by a wire at the leading-edge suggests that it thickens the boundary layer to a lesser extent than does the upper surface wire at 0·05 c; this is probably due to a favourable pressure gradient on the upper surface between the wire and the nose suction peak at the lower incidences.

9 CONCLUDING REMARKS

These tests, the first at the R.A.E. in which air was supplied to a model through the centre of a strain-gauge balance, showed the method to be a successful solution to the problem of introducing air without balance constraint.

The critical blowing momentum coefficient for attachment of flow over the flaps increases with flap angle as follows, at zero incidence. (The effect of incidence change is small.)

$\delta_{F,A}$	C'_{μ_a}
30°	0·015
45°	0·03
60°	0·05

In the presence of slipstream, the critical blowing momentum coefficient defined in terms of the velocity at the propeller disc was substantially independent of propeller thrust.

With increasing blowing momentum, the stall pattern changed from one of trailing-edge to leading-edge separation.

Increments of maximum lift coefficient obtained on the "clean" wing at a C'_μ of 0·1 were 0·65 and 1·82 respectively at flap angles of 0° and 60°, with intermediate values at intermediate flap angle.

ACKNOWLEDGEMENT

Whitworth Gloster Aircraft Ltd., now Hawker Siddeley Dynamics (Coventry) manufactured the model and provided staff to help with the test programme and the analysis of results.

Table 1

MODEL DATA

WING		
	Span	13·50 ft
	Aerodynamic mean chord $\bar{\bar{c}}$	1·405 ft
	Root chord (constant out to dihedral kink)	1·583 ft
	Tip chord	0·992 ft
	Gross area	18·60 sq ft
	Blown area	16·26 sq ft
	Aspect ratio	9·8
	Dihedral (outboard of kink)	4°
	Spanwise location of kink	2·033 ft
	Root section	NACA 64_2A_4 (16·5)
	Tip section	NACA 64_2A_4 (13)
	Wing twist	Zero
	Blowing slot depth (nominal)	0·0065 in. inboard of kink, tapered in proportion to chord
FLAP	Type	Plain
	Inner flap span (per side)	1·298 ft
	Inner edge from model centre line	0·735 ft
	Outer flap span (per side)	2·505 ft
	Flap chord/wing chord	0·25
AILERONS	Span (per side)	2·212 ft
	Aileron chord/wing chord	0·25
BODY	Overall length	8·317 ft
	Overall width	1·442 ft
	Overall depth	1·371 ft
PROPELLERS	Type	Single left-hand tractor
	Number of blades, each	4
	Diameter	1·60 ft
	Solidity	0·098
	Blade angle at 0·7 radius	17°
WING-BODY ANGLE		1°

Table 2

CONFIGURATIONS AND BLOWING RATES FOR FORCE AND MOMENT MEASUREMENTS

(a) Incidence range -5·5° to stall, unyawed model.

δ_F	δ_A	First series						Second series					
		C'_μ ≠											
		0	0·02	0·04	0·06	0·08	0·10	0	0·02	0·04	0·06	0·08	0·10
80	60	ϕ					ϕ	ϕ		ϕ			ϕ
	30	ϕ					ϕ	ϕ		ϕ			ϕ
	0	ϕ					ϕ	ϕ		ϕ			ϕ
	-28							ϕ		ϕ			ϕ
60	60	ϕ			ϕ		ϕ	ϕ	ϕ	ϕ	ϕ	ϕ	ϕ
	45							ϕ		ϕ			ϕ
	30	ϕ			ϕ		ϕ	ϕ	ϕ	ϕ	ϕ	ϕ	ϕ
	15							ϕ		ϕ			ϕ
	0	ϕ			ϕ		ϕ	ϕ	ϕ	ϕ	ϕ	ϕ	ϕ
	-15							ϕ		ϕ			ϕ
	-28							ϕ	ϕ	ϕ	ϕ	ϕ	ϕ
45	60							ϕ		ϕ			ϕ
	45	ϕ		ϕ	ϕ		ϕ	ϕ	ϕ	ϕ	ϕ	ϕ	ϕ
	30							ϕ		ϕ			ϕ
	0	ϕ		ϕ			ϕ	ϕ		ϕ			ϕ
	-28							ϕ		ϕ			ϕ
30	60	ϕ	ϕ		ϕ		ϕ	ϕ		ϕ			ϕ
	30	ϕ	ϕ		ϕ		ϕ	ϕ	ϕ	ϕ	ϕ	ϕ	ϕ
	0	ϕ	ϕ				ϕ	ϕ	ϕ	ϕ	ϕ	ϕ	ϕ
	-28							ϕ		ϕ			ϕ
0	60	ϕ	ϕ				ϕ	ϕ	ϕ	ϕ	ϕ	ϕ	ϕ
	45							ϕ		ϕ			ϕ
	30							ϕ	ϕ	ϕ	ϕ	ϕ	ϕ
	15							ϕ		ϕ			ϕ
	0							ϕ	ϕ	ϕ	ϕ	ϕ	ϕ
	-15							ϕ		ϕ			ϕ
	-28							ϕ	ϕ	ϕ	ϕ	ϕ	ϕ

≠ Nominal value of C'_μ. Actual value may differ by ±0·002

ϕ Indicates measurements made at this condition.

Table 2 (Contd.)

(b) Yaw range ±20°, at α = 0°, 3°, 6°, 9°

First series only

δ_F	δ_A	C'_μ †				
		0	0·02	0·04	0·06	0·10
80	30	ϕ				$\phi^{(9)}$
80	0	ϕ				$\phi^{(9)}$
60	60	ϕ			ϕ	ϕ
60	30	ϕ			ϕ	$\phi^{(9)}$
60	0	$\phi^{(3)}$				
45	45	$\phi^{(3)}$		$\phi^{(3)}$	$\phi^{(3)}$	$\phi^{(3,9)}$
45	0			$\phi^{(3,9)}$		$\phi^{(3,9)}$
30	30	ϕ	ϕ			ϕ
30	0	$\phi^{(3)}$	$\phi^{(3)}$			$\phi^{(3)}$
0	0	$\phi^{(3)}$				$\phi^{(3)*}$

ϕ Indicates measurements at this condition

Figures in brackets indicate incidence omitted

* Additional incidence, α = +12°.

(c) Incidence range -5·5° to stall. Unyawed model. Aileron differential runs

δ_{AP}	δ_{AS}	First series		Second series	
		δ_F = 0 C'_μ = 0, 0·02, 0·1 †	δ_F = 60 C'_μ = 0, 0·06, 0·1 †	δ_F = 0 C'_μ = 0 and 0·1 †	δ_F = 60
-28	30	ϕ		ϕ	
-15	15	ϕ			
15	-15	ϕ			
30	-28	ϕ			
0	-28	ϕ		ϕ	ϕ
0	-15			ϕ	ϕ
0	15			ϕ	ϕ
0	30	ϕ		ϕ	ϕ
0	45			ϕ	ϕ
0	60		ϕ	ϕ	ϕ
15	45		ϕ		
45	15		ϕ		
60	0		ϕ		

† Nominal value. Actual value may differ by ±0·002.

Table 2 (Contd.)

(d) Tests with slipstream

δ_F	δ_A	T_c	C_μ †
60	60	0	0, 0·1, 0·25
		0·8	0, 0·1
		1·4	0, 0·1, 0·156
		1·8	0, 0·1, 0·156
		2·56	0·178
		4·1	0·229
60	0	0	0, 0·1
		0·8	0, 0·1
		1·4	0, 0·1, 0·156
		1·8	0, 0·1, 0·156
		2·56	0·177
		4·1	0, 0·228
60	30	0	0, 0·1, 0·25
		0·8	0, 0·1
		1·8	0, 0·1, 0·156
		4·1	0, 0·229
30	30	0	0, 0·1
		0·8	0, 0·1
		1·8	0, 0·1
0	0	0	0
		0·8	0
		1·8	0
		4·1	0

† Nominal values. Actual values may differ by ±0·002

SYMBOLS

α	=	wing incidence (chord line to free stream direction)	
δ_F	=	flap deflection	
δ_A	=	aileron deflection, equal for both ailerons	
$\delta_{F,A}$	=	deflection of flap and aileron, where these are equal	
δ_{A_P}	=	deflection of port aileron	
δ_{A_S}	=	deflection of starboard aileron (all control angles positive for downward deflection)	
y	=	lateral distances from centre line	ft
b	=	wing span	ft
z	=	distance from local surface, normal to the surface	ft
c	=	local chord	ft
$\bar{\bar{c}}$	=	aerodynamic mean chord $\left(= \frac{\int c^2\, dy}{\int c\, dy}\right)$	ft
S	=	wing area ($= \int c\, dy$ over the span)	ft^2
S'	=	blown wing area ($= \int c\, dy$ over the span of the blowing slots)	ft^2
D	=	propeller diameter	ft
ρ_o	=	free stream air density	$slug/ft^3$
V_o	=	free stream velocity	ft/s
q_o	=	free stream dynamic head ($= \frac{1}{2} \rho_o V_o^2$)	lb/ft^2

$$C_L = \frac{\text{Lift}}{q_o S} \qquad C_D = \frac{\text{Drag}}{q_o S} \qquad C_Y = \frac{\text{Sideforce}}{q_o S}$$

$$C_m = \frac{\text{Pitching moment}}{q_o S \bar{\bar{c}}} \qquad C_n = \frac{\text{Yawing moment}}{q_o S b} \qquad C_\ell = \frac{\text{Rolling moment}}{q_o S b}$$

(moments being given about "yawed wind axes", i.e. mutually perpendicular axes lying in or normal to the vertical plane containing the model centre line, and the horizontal plane. These axes intersect at a point on the centre line root chord and in the transverse plane of the quarter chord point of the aerodynamic mean chord).

p	=	local static pressure	lb/ft^2
p_o	=	free stream static pressure	lb/ft^2

SYMBOLS (Contd.)

$C_p = \dfrac{p - p_o}{q_o}$

T_c = propeller thrust coefficient $\left(= \dfrac{\text{Thrust}}{\rho V_o^2 D^2} \right)$

m = mass flow rate of blowing air — slug/s

V_J = velocity of blowing air, assuming adiabatic expansion to static pressure p_o — ft/s

$C_\mu = \dfrac{m V_j}{q_o S}$ $\quad C'_\mu = \dfrac{m V_j}{q_o S'}$ blowing momentum coefficients

C'_{μ_a} = minimum value of C'_μ required to maintain attached flow

C_H = control hinge moment coefficient =

$$\frac{\text{control hinge moment}}{q_o \times (\text{control area}) \times (\text{control mean chord})}$$

a = propeller inflow coefficient. Velocity at propeller disc = $V_o (1 + a)$

h = total head pressure — lb/ft^2

REFERENCES

No.	Author	Title, etc.
1	R. C. W. Eyre	Description of model and test rig for flap blowing tests with slipstream in the 24 ft wind tunnel. R.A.E. Technical Note Aero 2919 (A.R.C. 25596) (1963)
2	J. Williams S. F. J. Butler	Aerodynamic aspects of boundary-layer control for high lift at low speeds. R.A.E. Technical Note Aero 2858 (A.R.C. 24535) (1962)
3	R. Smelt H. Davies	Estimation of increase in lift due to slipstream. A.R.C. R. & M. 1788 (1936)

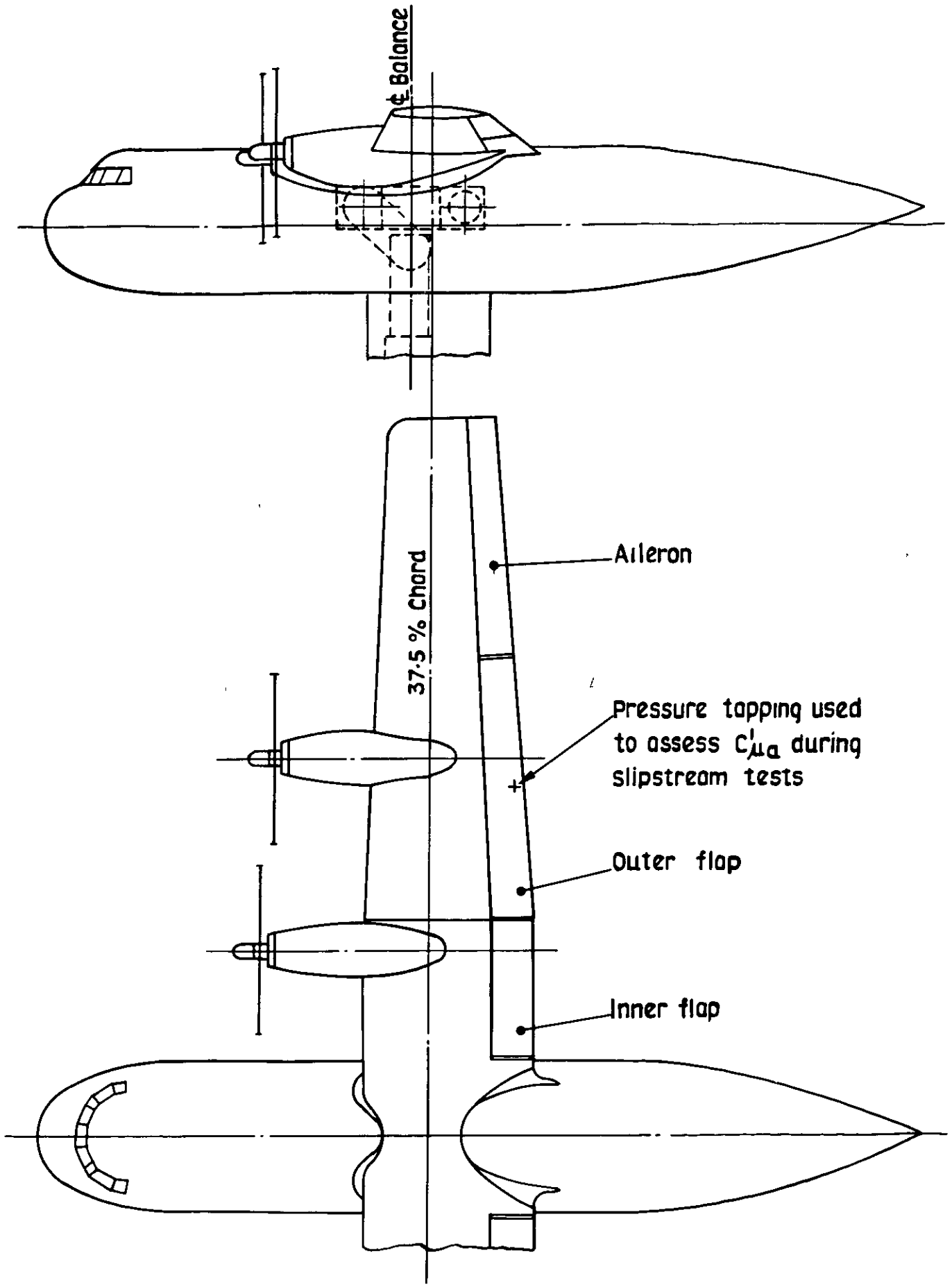

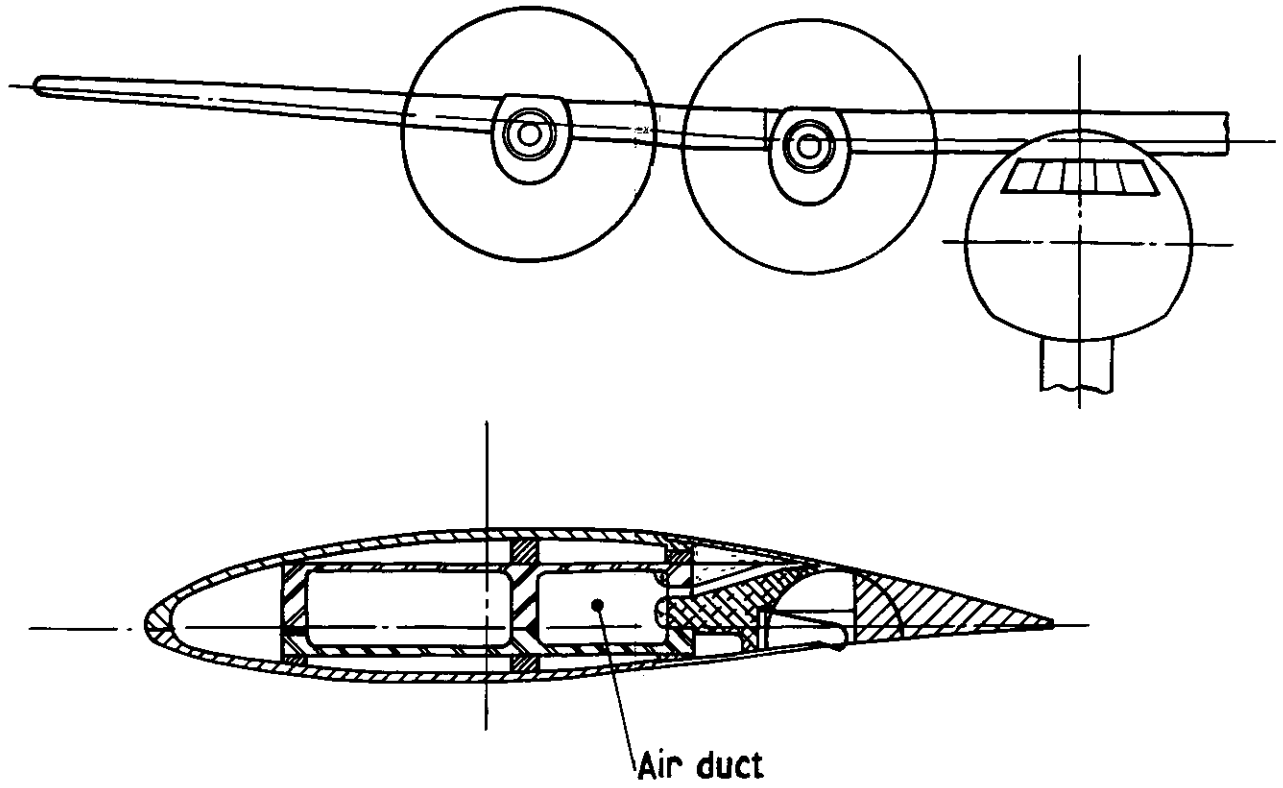

Fig. 1 General Arrangement of model and details of blowing slot

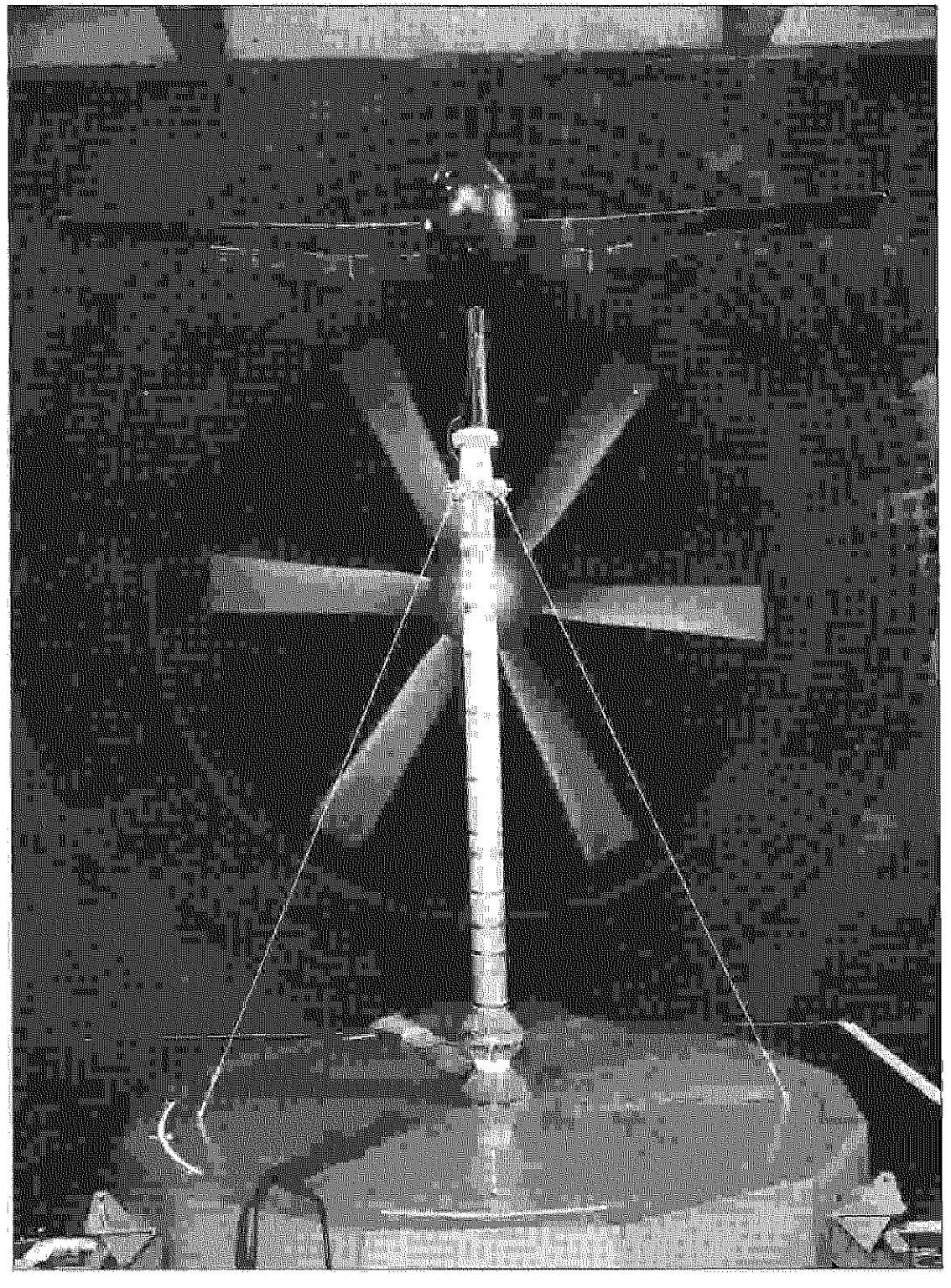

Fig.2 Model in 24ft. wind tunnel

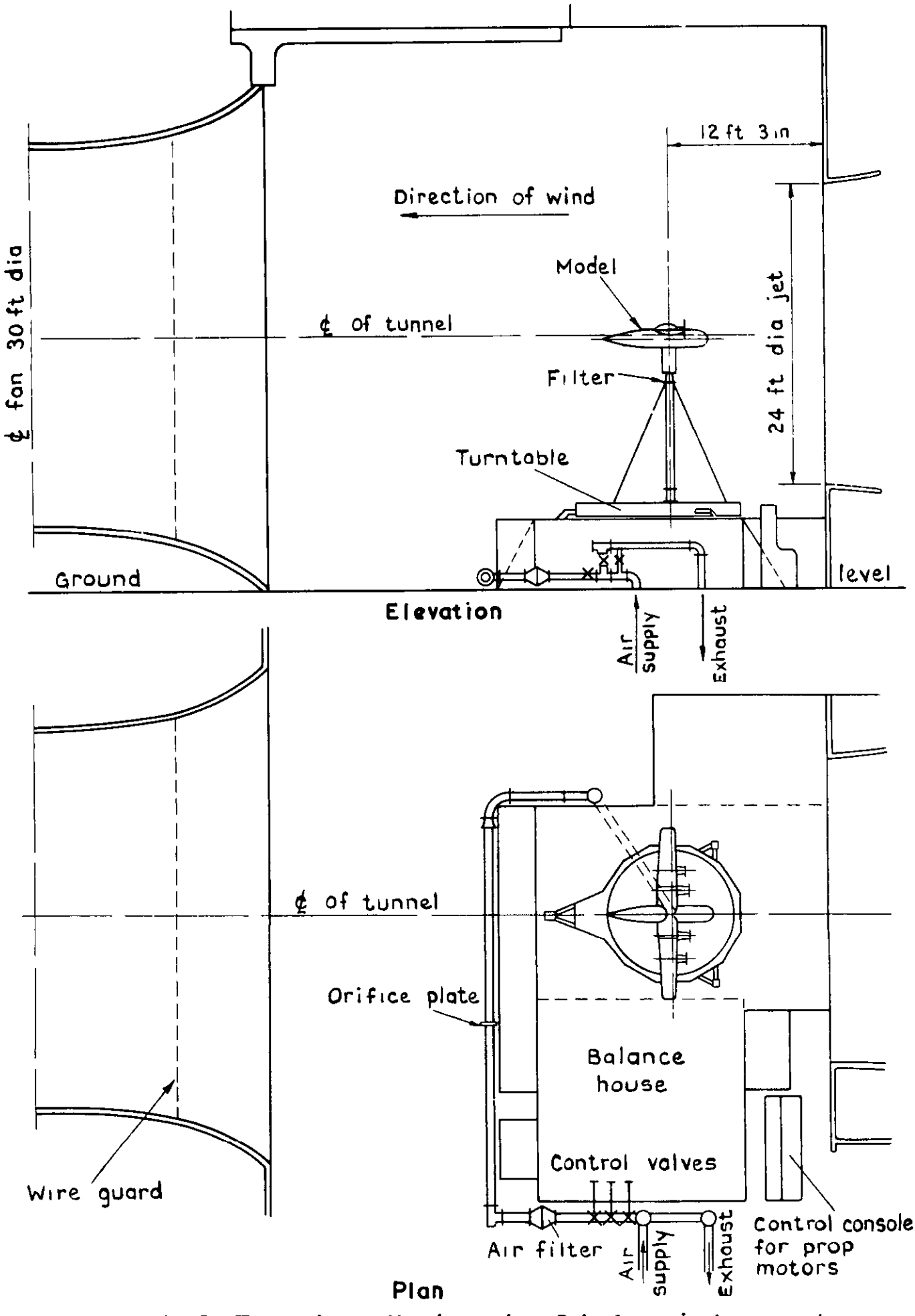

Fig.3 Test installation in 24 ft wind tunnel

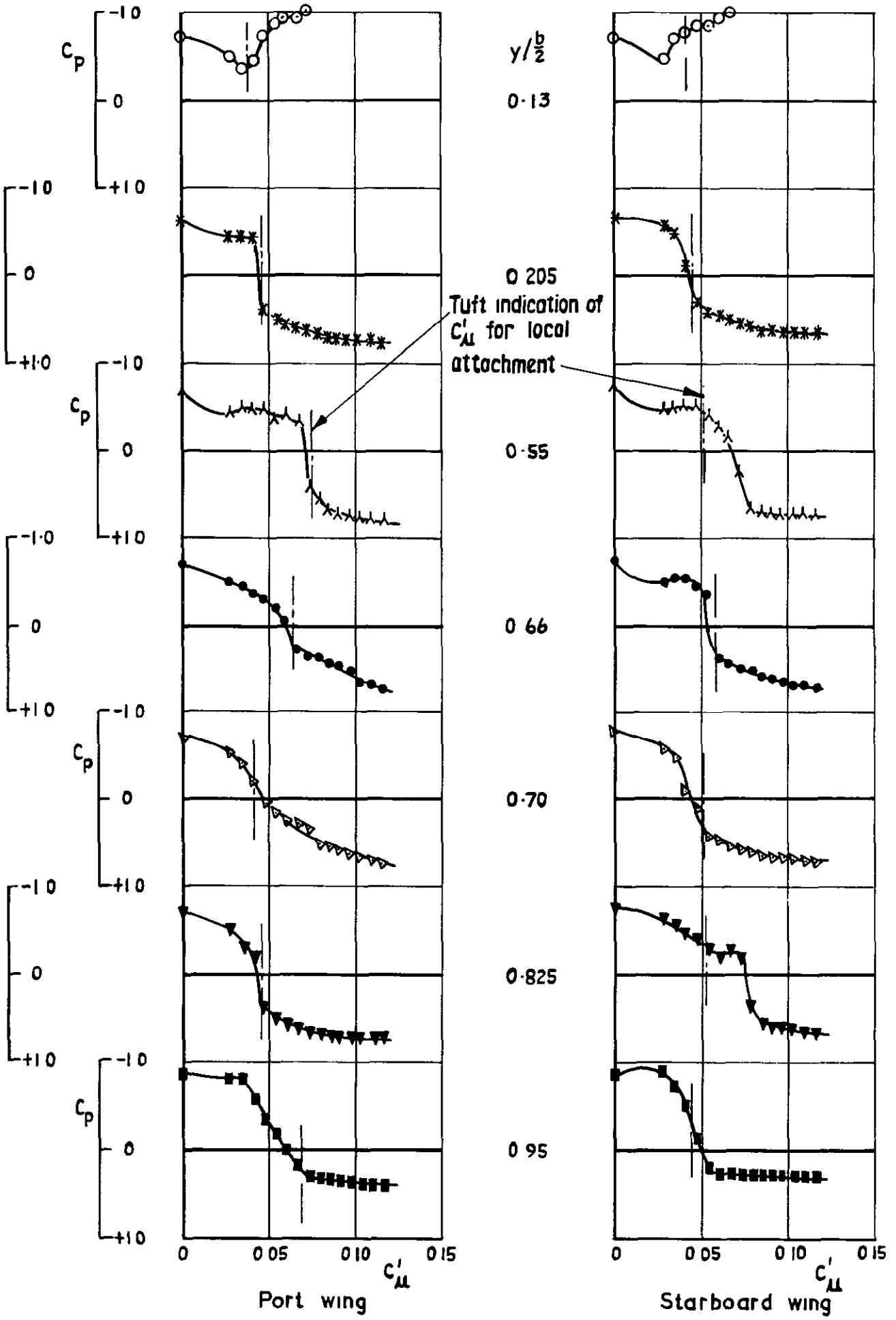

Fig 4 Comparison of tuft indication of attachment and C_p vs C'_μ curves Second series Pressures at T E $\delta_F = \delta_A = 60^\circ$ $\alpha_W = 0^\circ$

Symbol	$y/\frac{b}{2}$
⊙	0·15
✱	0 25
▽	0 35
◇	0·495
Y	0 625
+	0 71
□	0·80
X	0 905
○	0·935

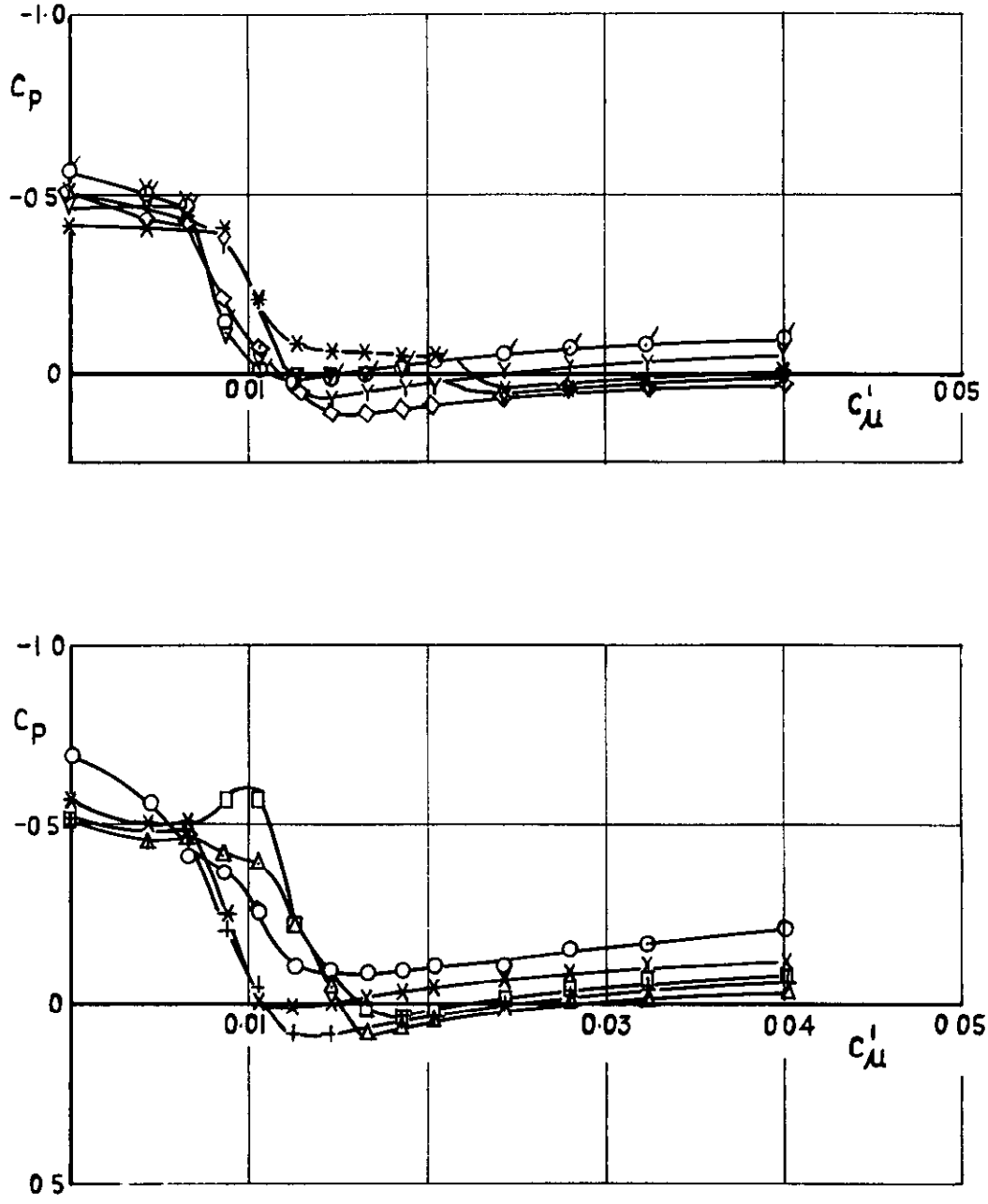

Fig 5 C_p vs C'_μ $\delta_F = \delta_A = 30°$ Starboard wing. $\alpha = 0°$
First series Pressures at 0 95c on upper surface

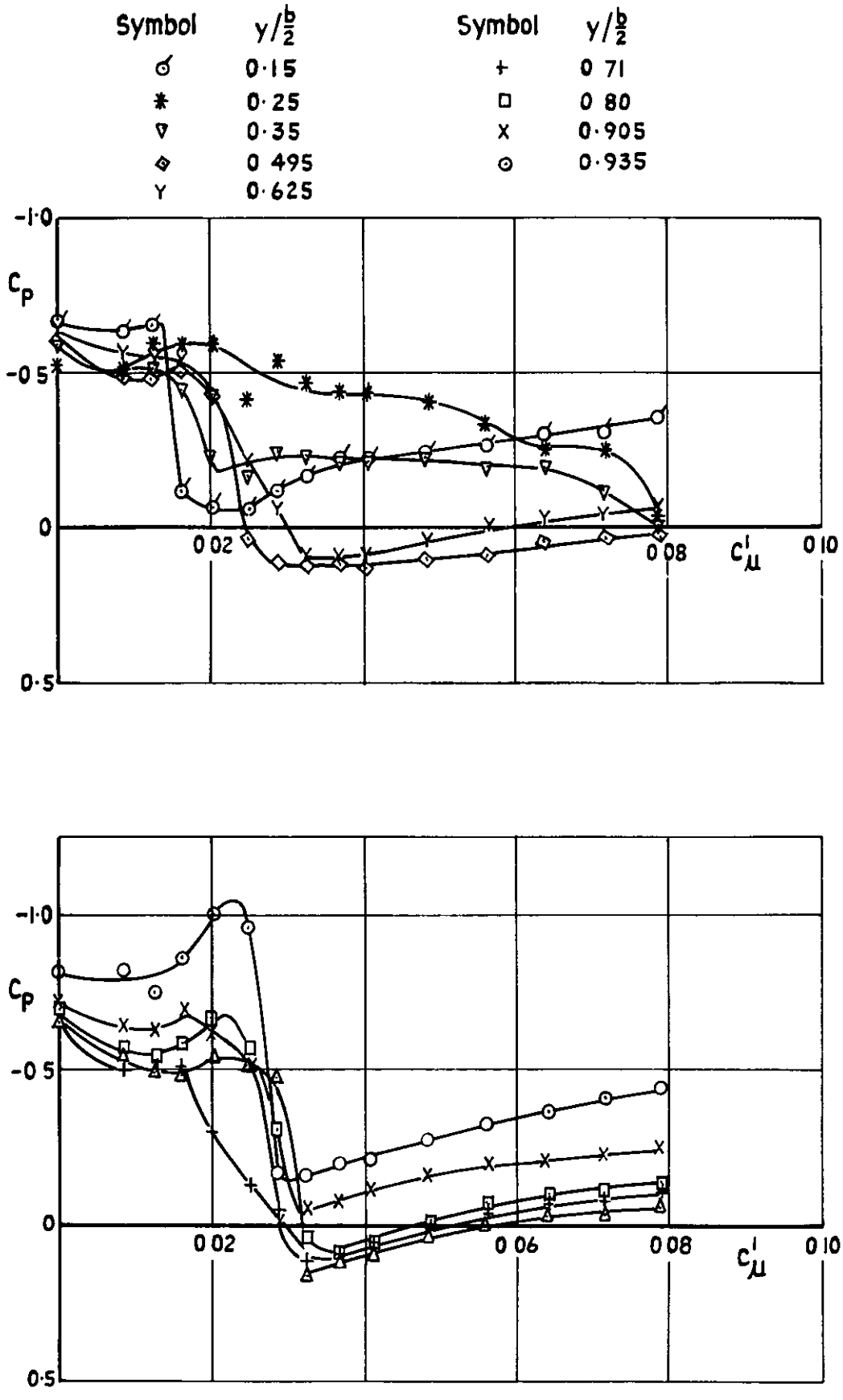

Fig 6 C_p vs C_μ' $\delta_F = \delta_A = 45°$ Starboard wing. $\alpha = 0°$
First series Pressures at O 95c on upper surface

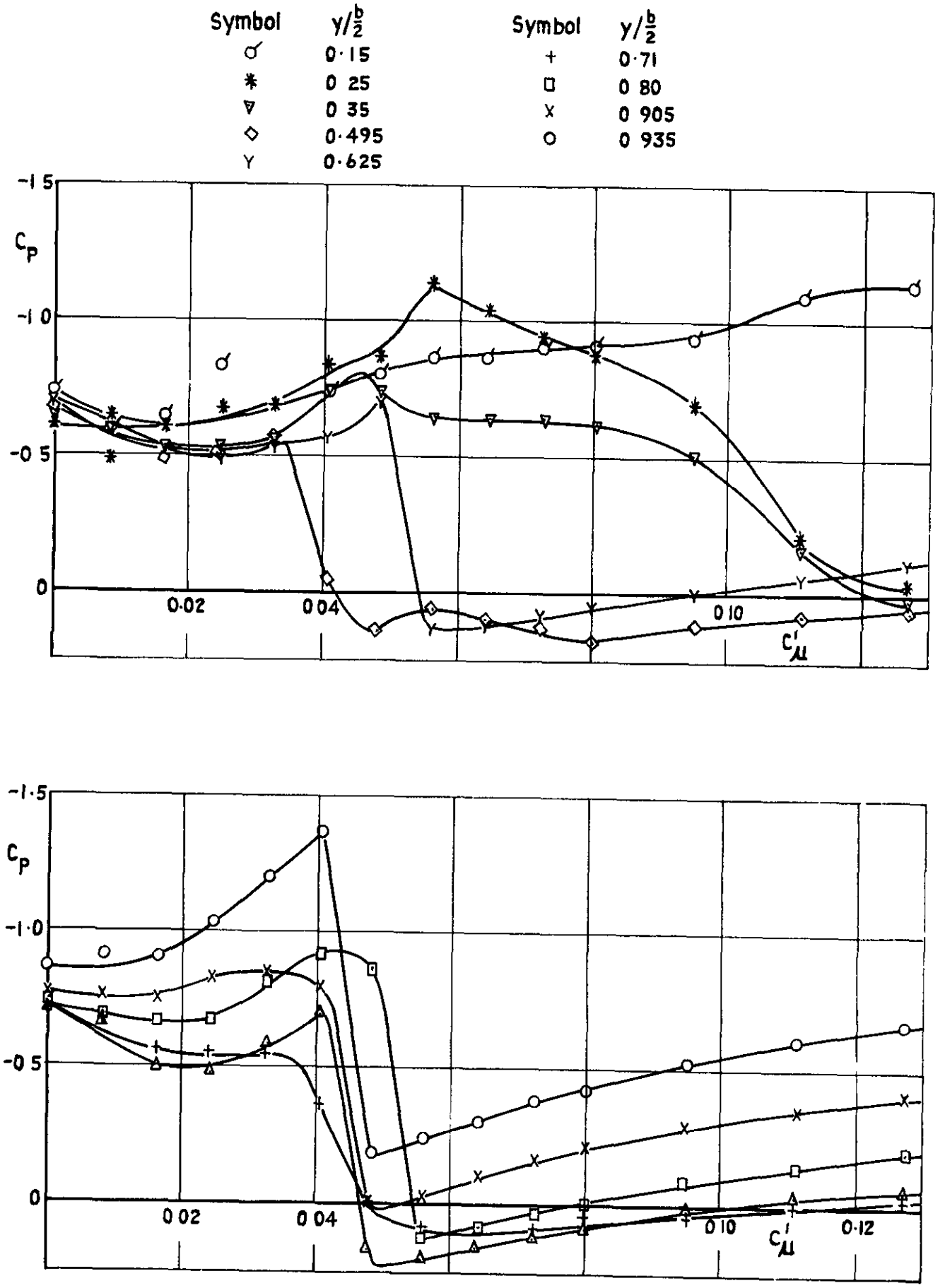

Fig. 7 C_p vs C_μ' $\delta_F = \delta_A = 60°$ Starboard wing. $\alpha = 0°$
First series Pressures at 0 95c on upper surface

Symbol	$y/\frac{b}{2}$	$\frac{x}{c}$	Symbol	$y/\frac{b}{2}$	$\frac{x}{c}$	Symbol	$y/\frac{b}{2}$	$\frac{x}{c}$
⊙	0 13	1 0	⅄	0·55	1·0	♂	0 15	0 95
✱	0·205	1·0	●	0 66	1·0	▽	0·35	0 95
⊡	0·285	1·0	▷	0 70	1·0			
Y	0 30	1·0	▼	0·825	1·0			
▲	0·32	1·0	■	0 95	1·0			
◇	0·435	1·0						

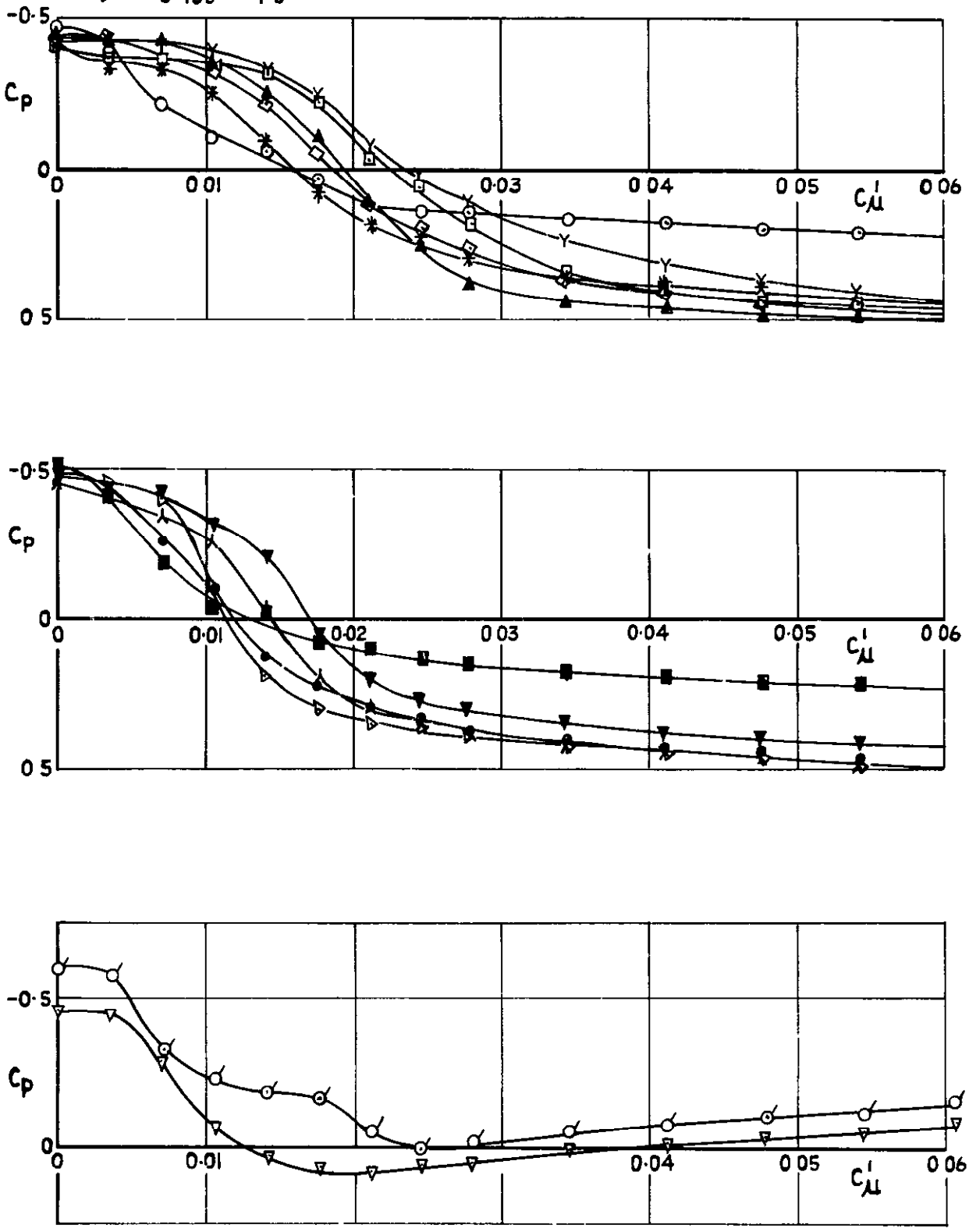

Fig. 8 C_p vs C_μ' $\delta_F = \delta_A = 30°$ Starboard wing. $\alpha = 0°$

Second series

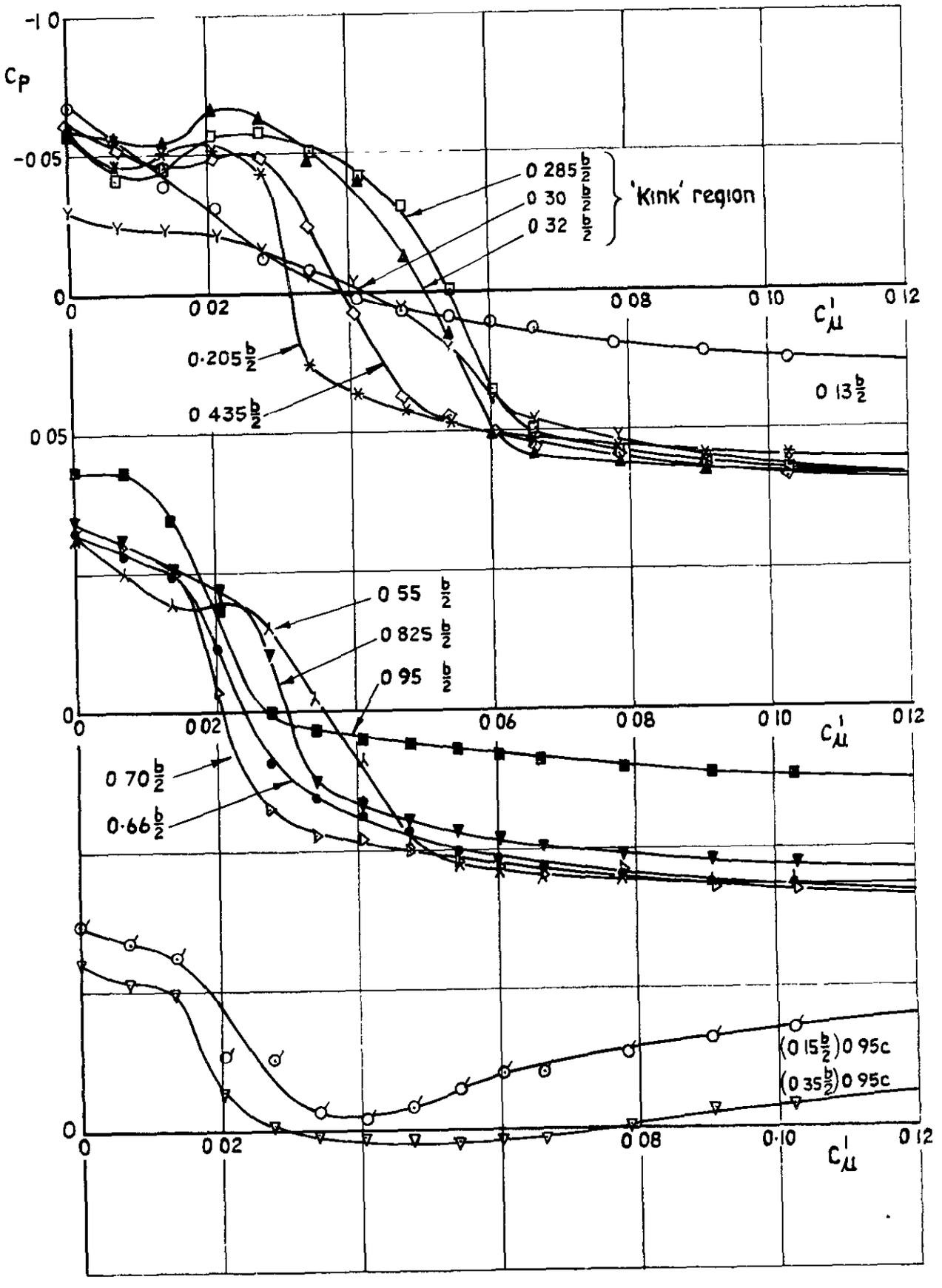

Fig 9 C_p vs C'_μ $\delta_F = \delta_A = 45°$ Starboard wing. $\alpha = 0°$

Second series

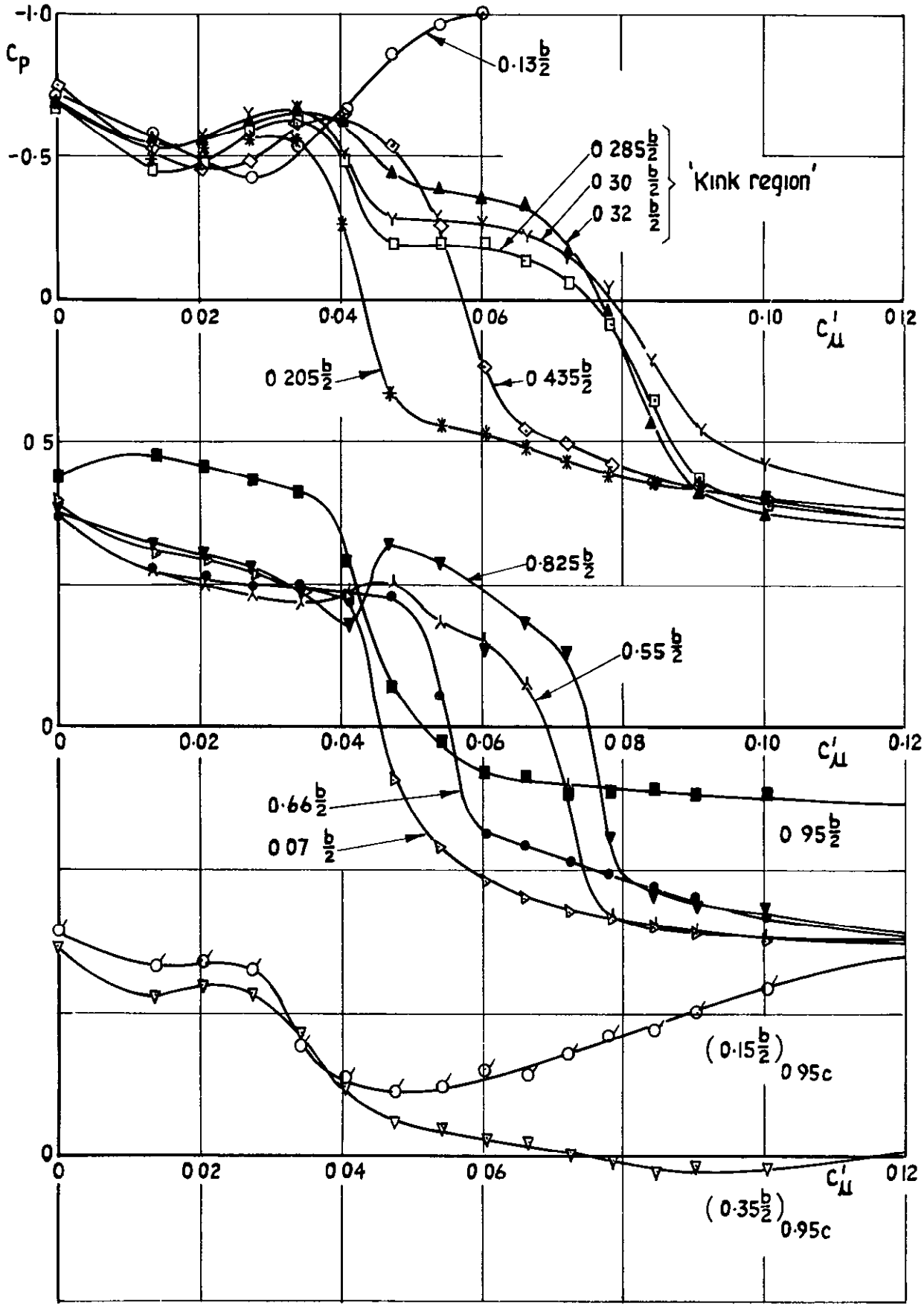

Fig 10 C_p vs C'_μ $\delta_F = \delta_A = 60°$ Starboard wing . $\alpha = 0°$
Second series

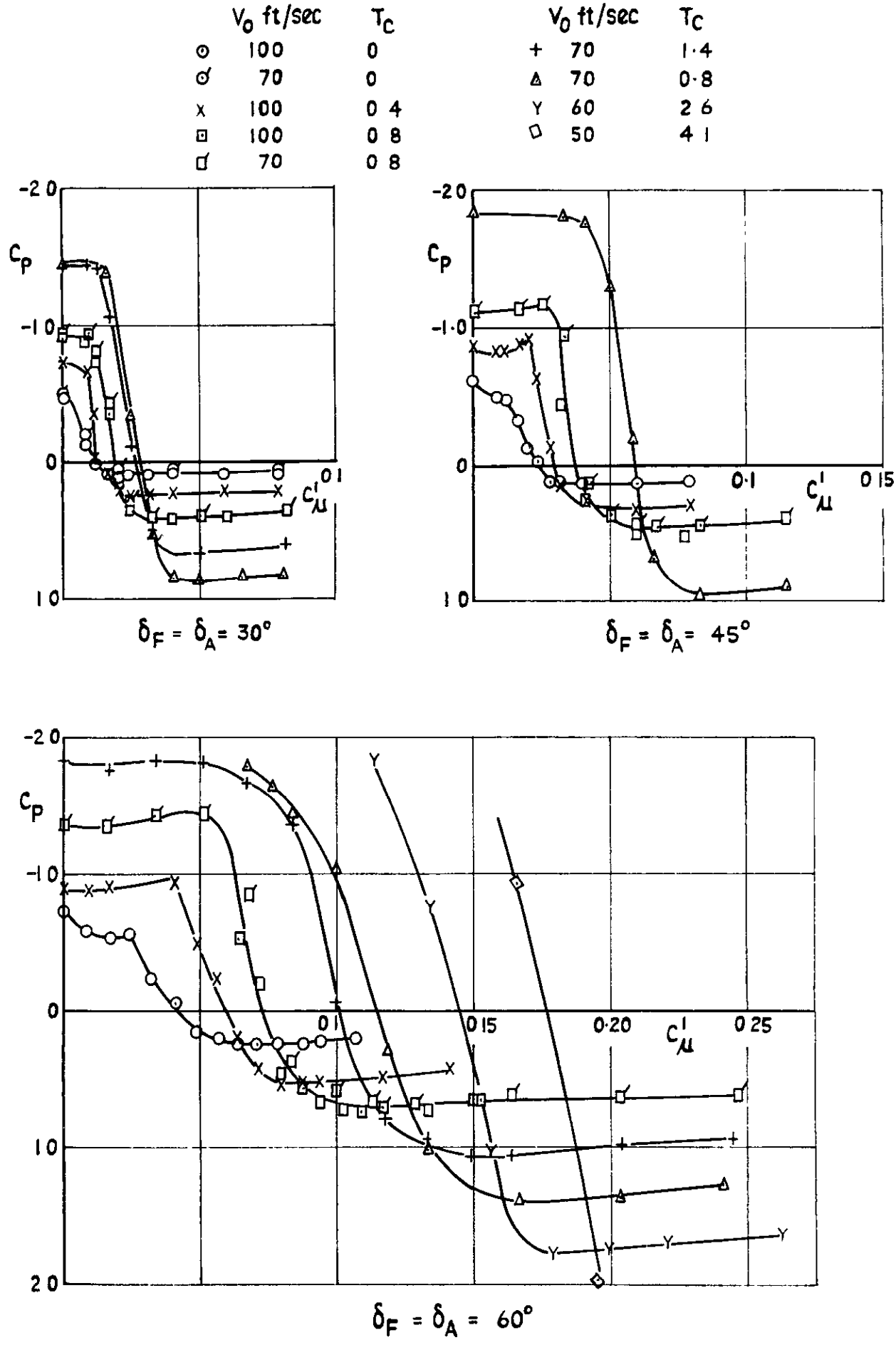

Fig. 11 C_p vs C'_μ with slipstream at $y = 0\ 495\ \frac{b}{2}$ $x = 0\ 95c$ on upper surface of starboard wing $\alpha = 0°$

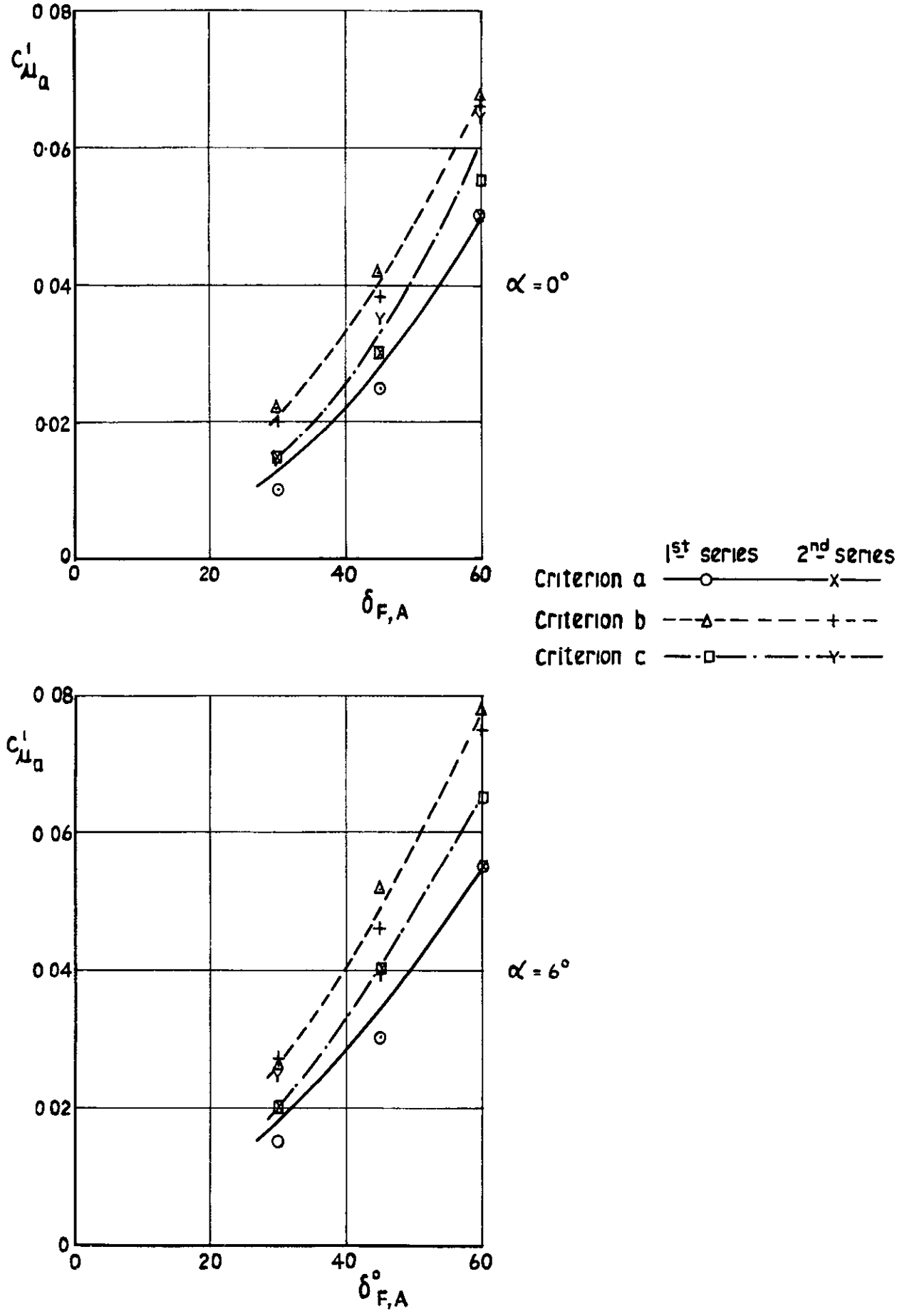

'Clean' wing without slipstream

Fig. 12a Critical blowing coefficients

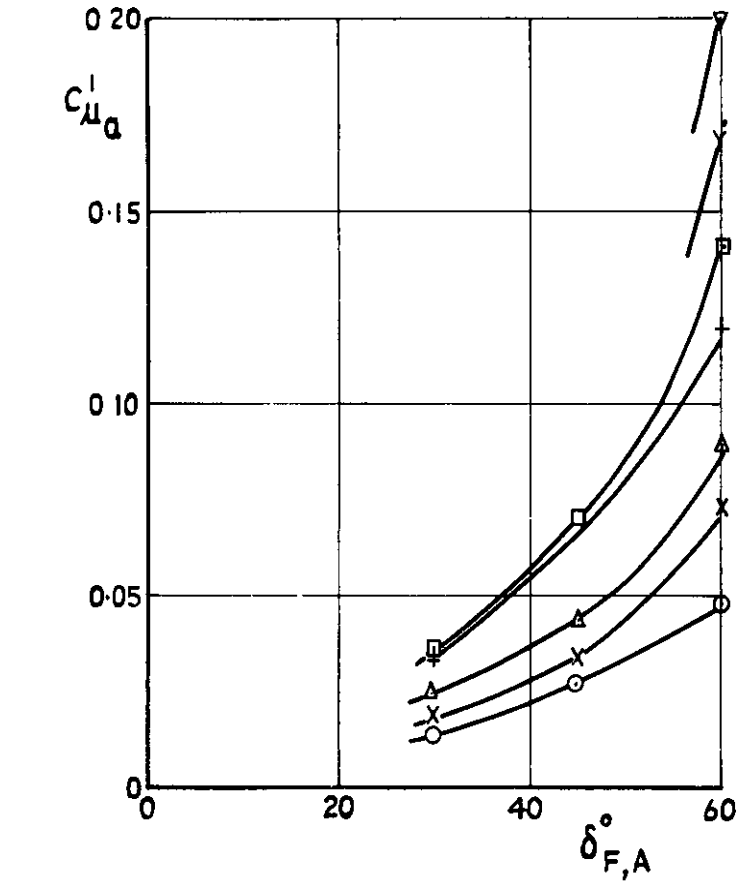

T_c	Symbol
0	○
0 4	×
0 8	△
1·4	+
1 8	□
2 6	Y
4 1	▽

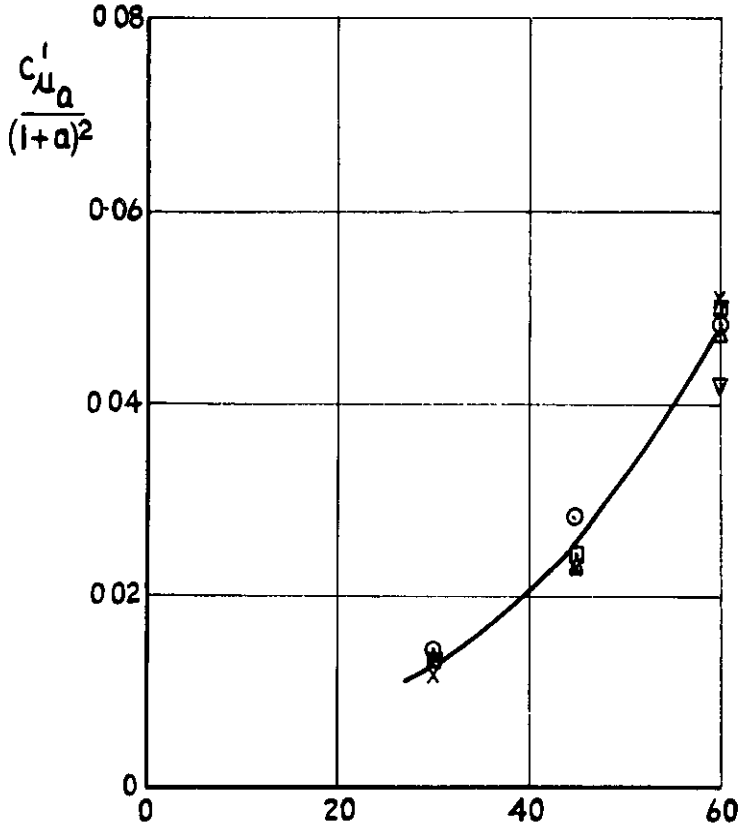

With slipstream $\alpha = 0^\circ$ Criterion a

Fig 12b Critical blowing coefficients

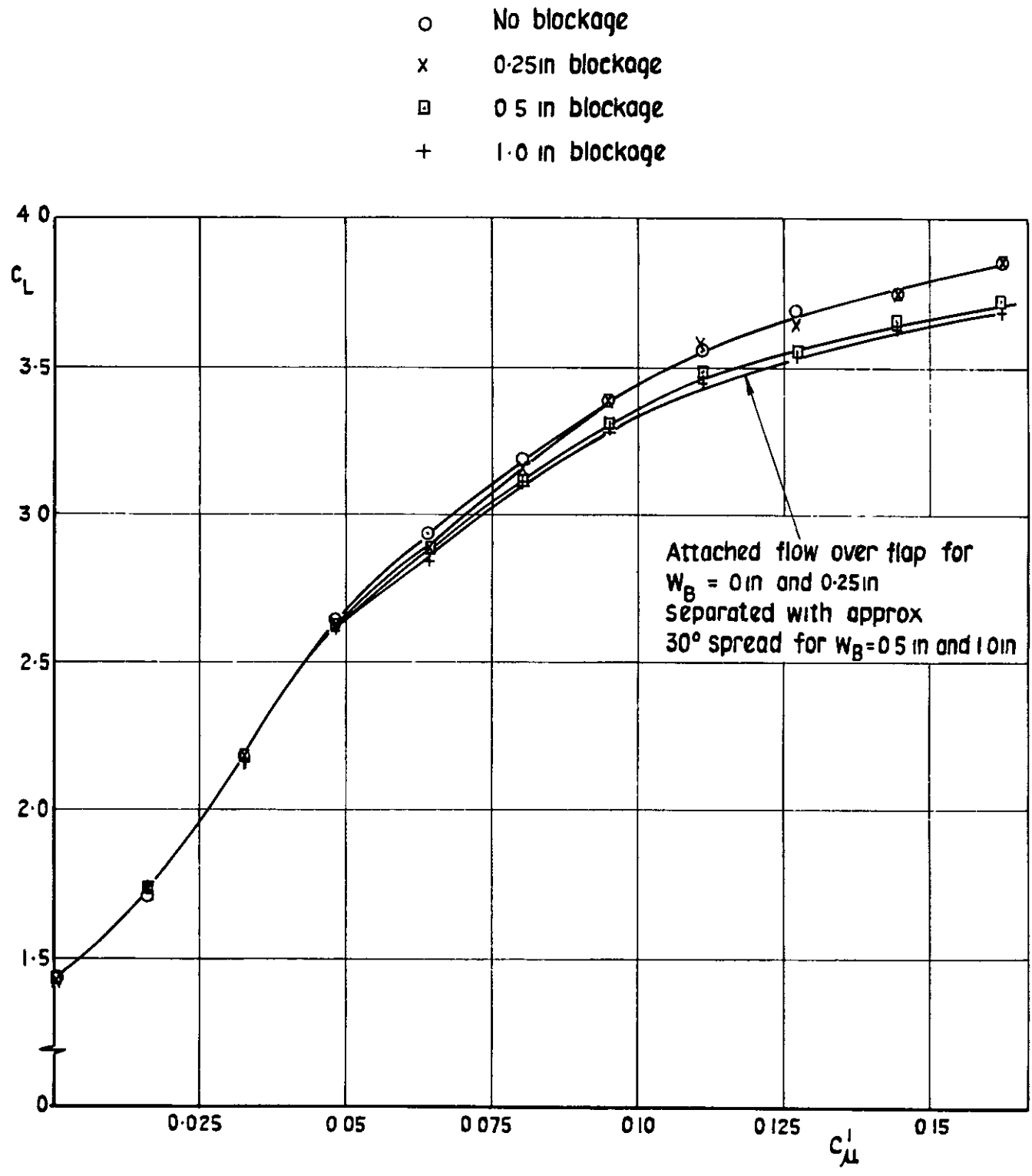

Fig 13 C_L vs C'_μ with small blockage in blowing slot (ahead of starboard outer flap)

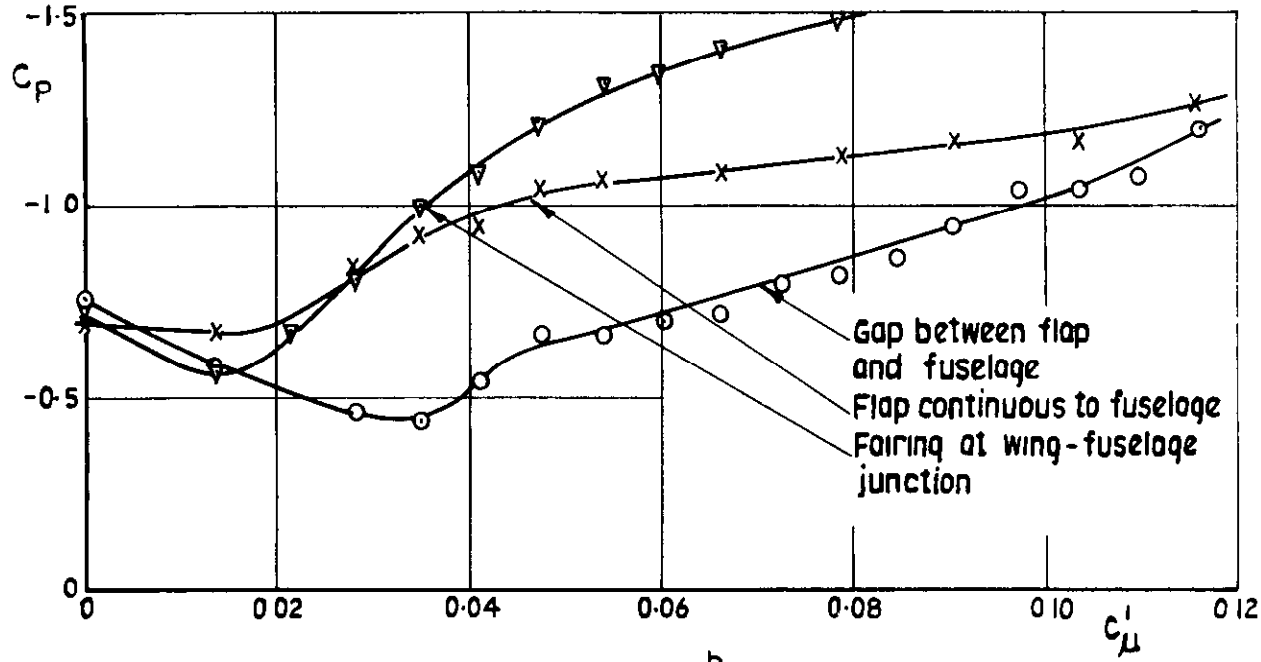

a $y = 0\ 13\ \frac{b}{2}$

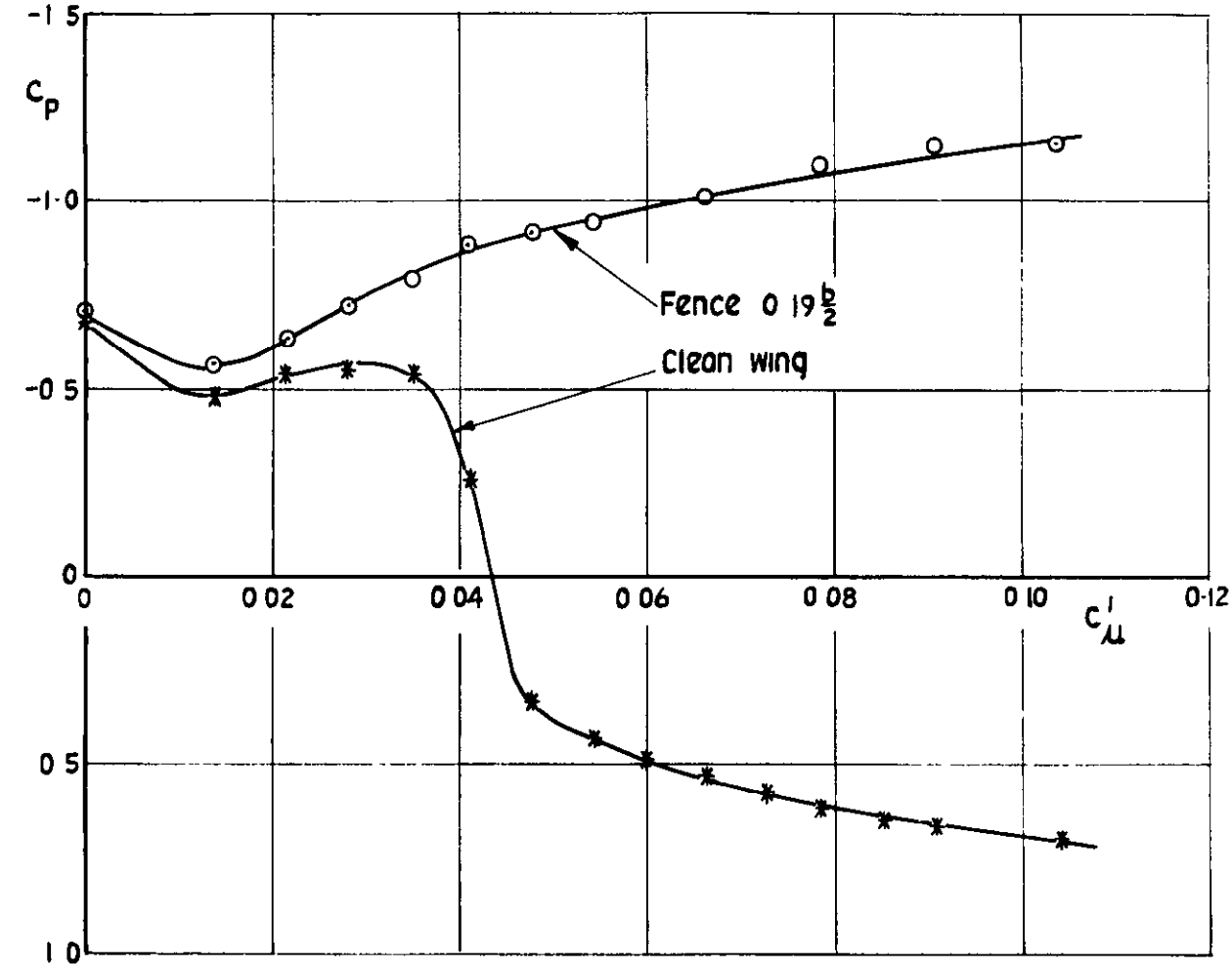

b $y = 0\ 205\ \frac{b}{2}$

Fig 14a & b C_p vs C'_μ near the fuselage junction
Starboard wing $\delta_F = \delta_A = 60°$ $\alpha = 0°$

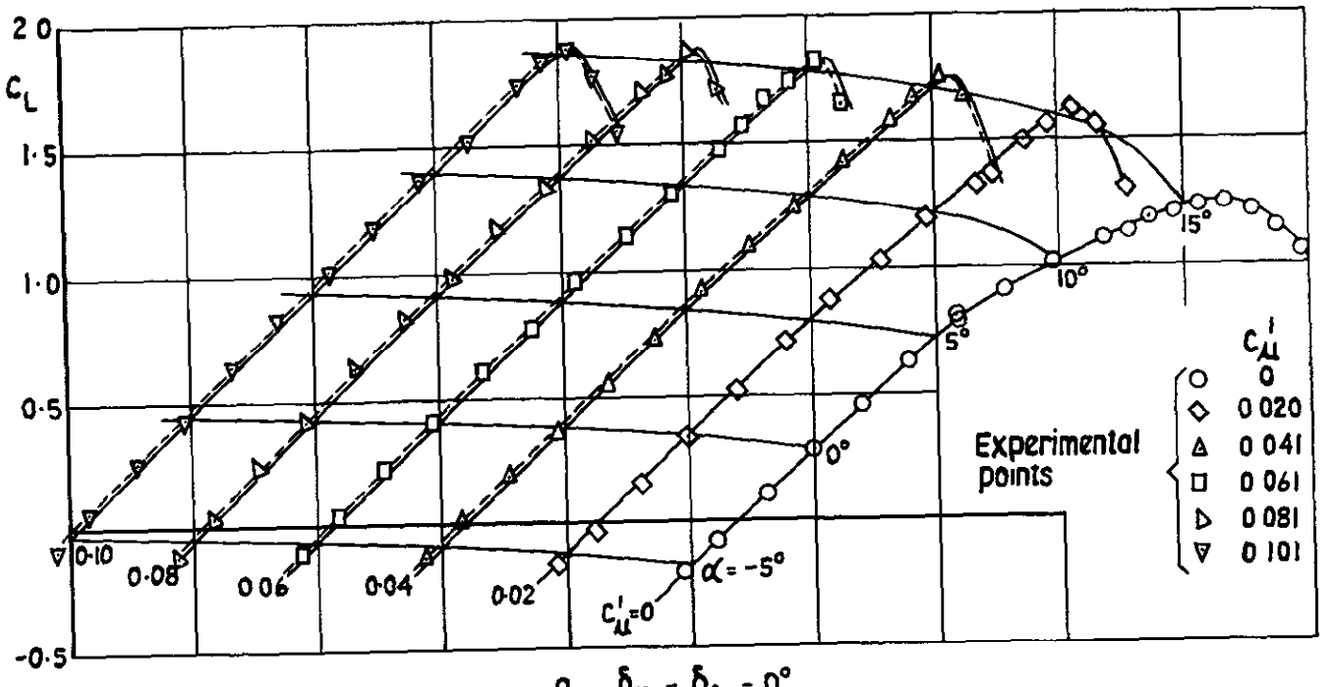

a $\delta_F = \delta_A = 0°$

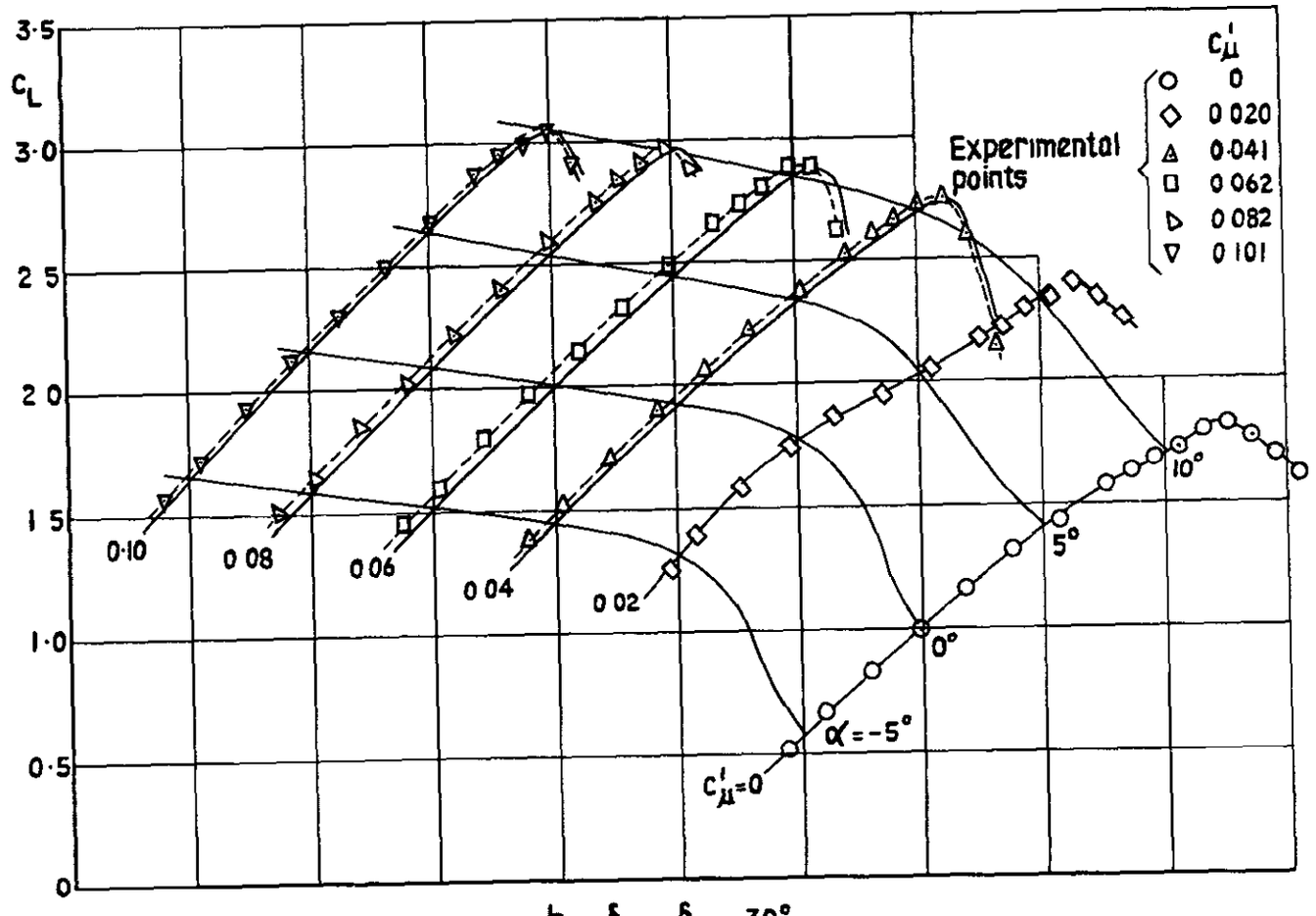

b $\delta_F = \delta_A = 30°$

Fig 15a & b Variation of C_L with α and C'_μ Second series

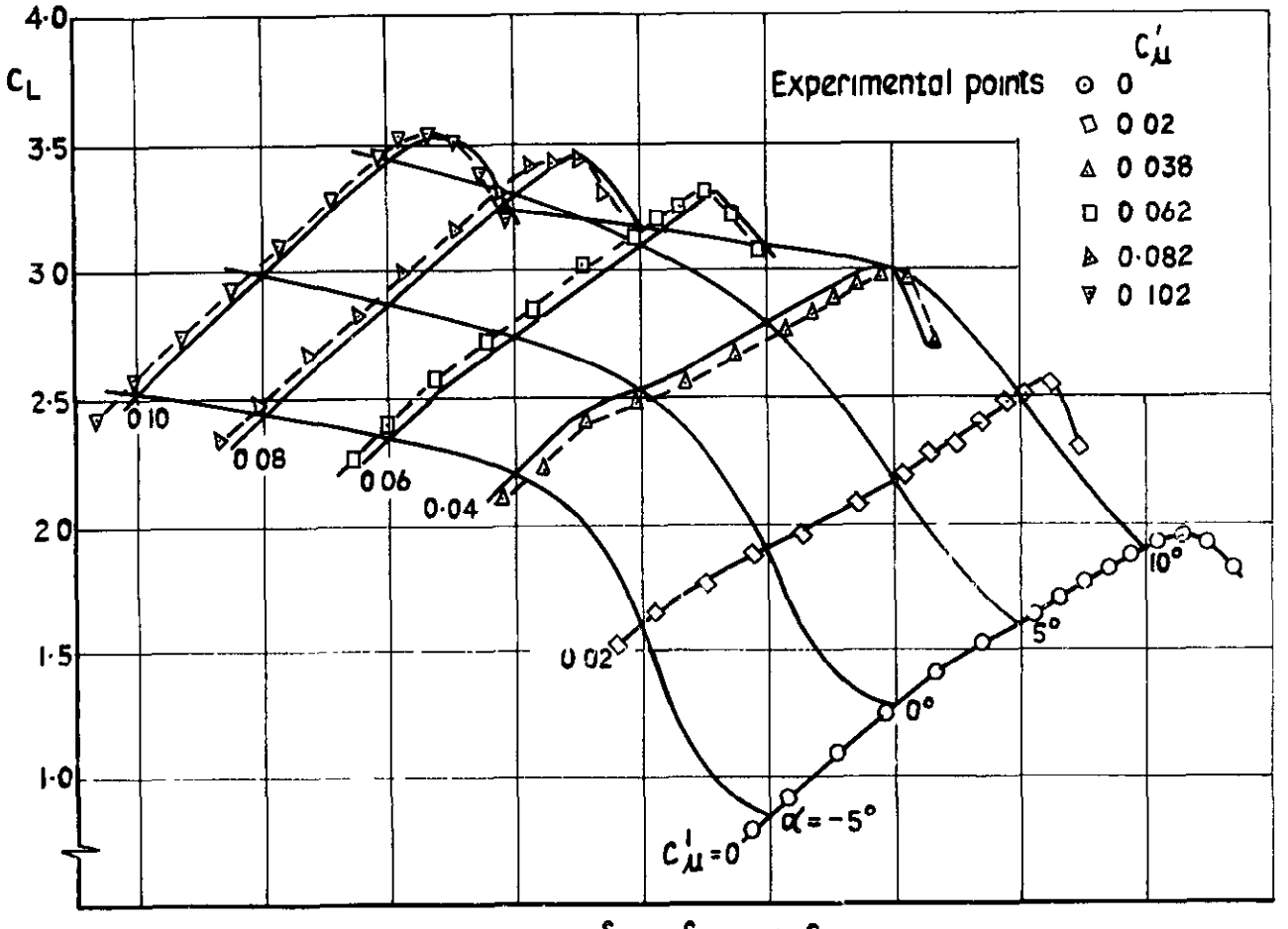

c $\delta_F = \delta_A = 45°$

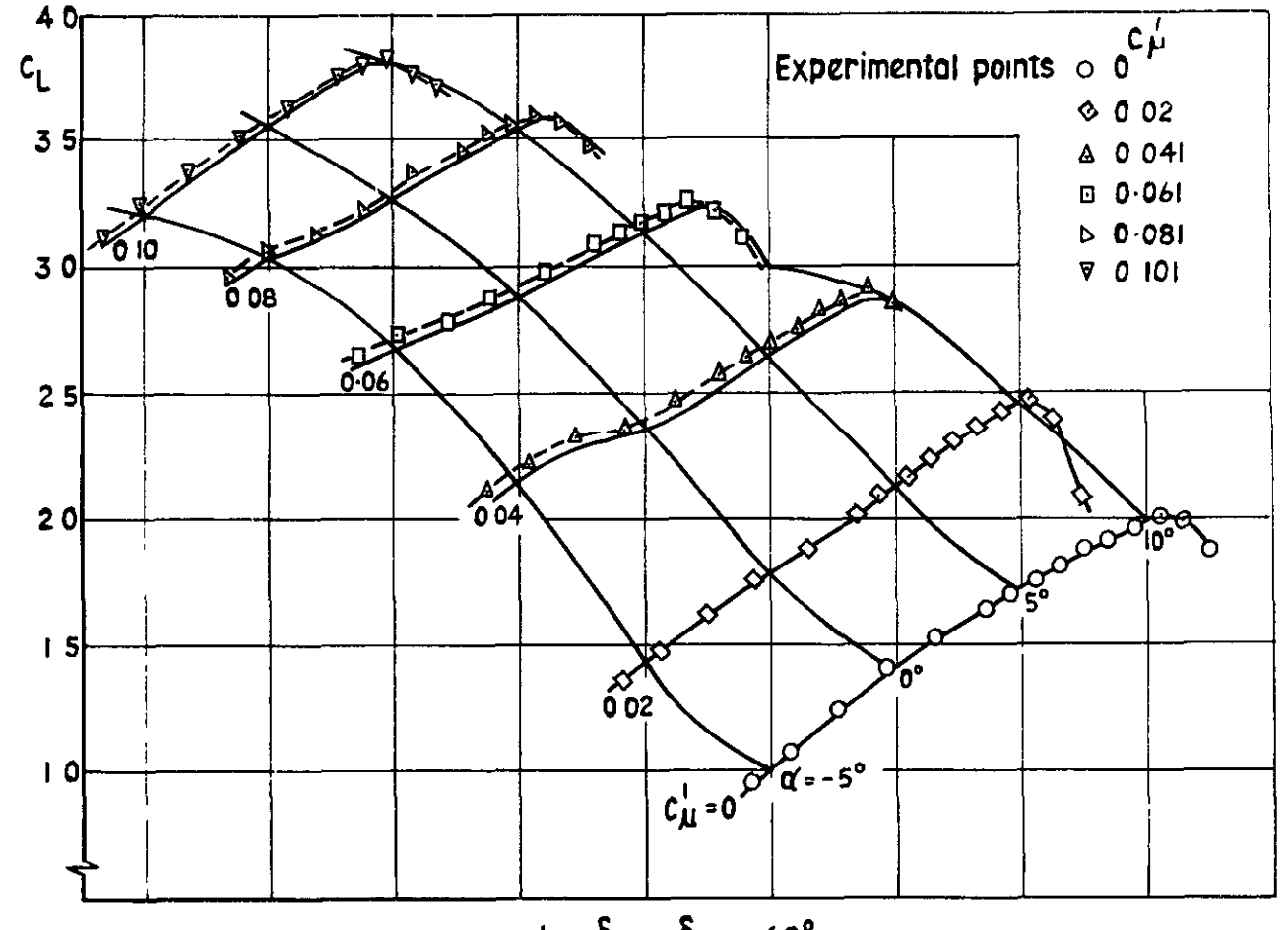

d $\delta_F = \delta_A = 60°$

Fig. 15c & d Variation of C_L with α and C'_μ

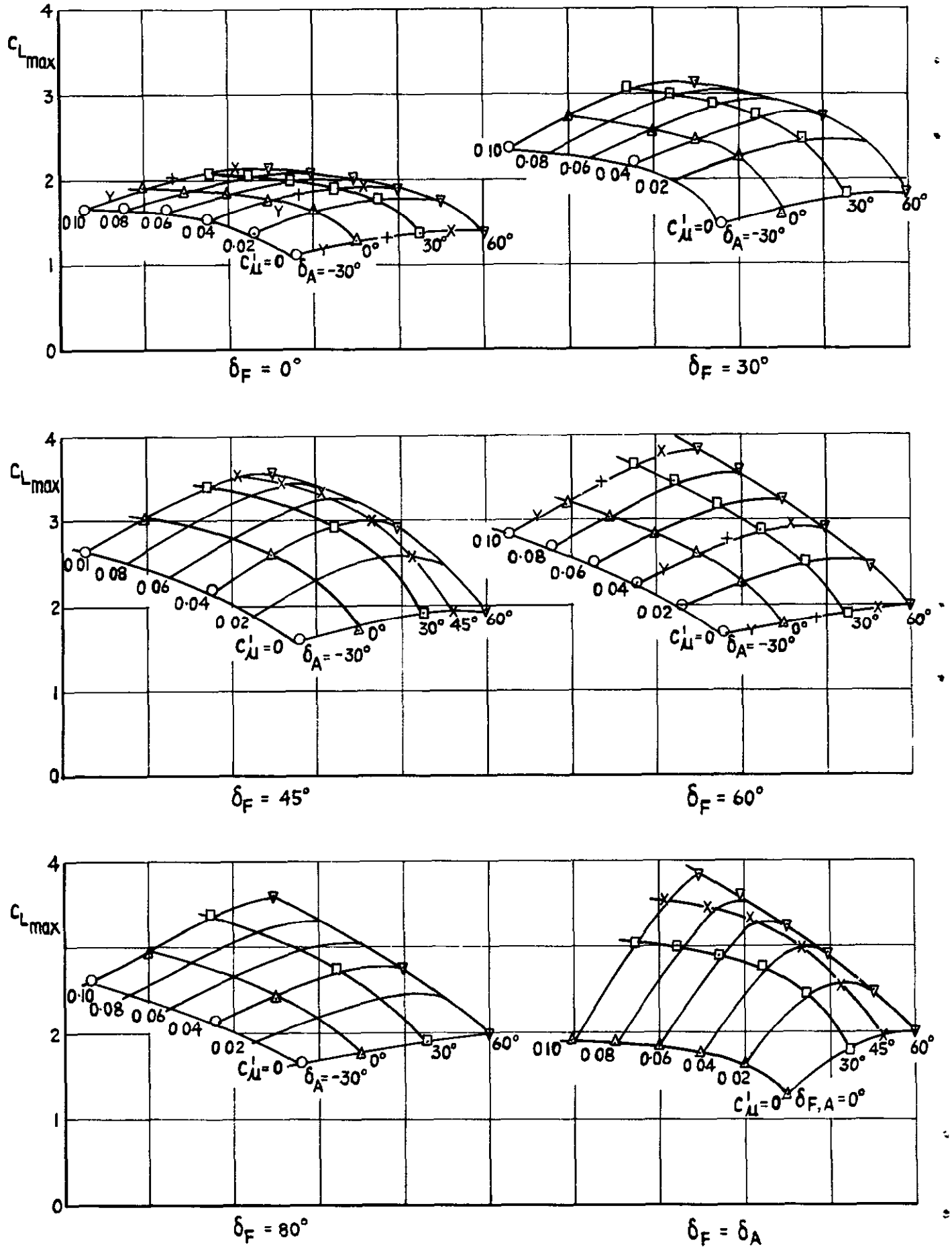

Fig 16 Maximum values of C_L

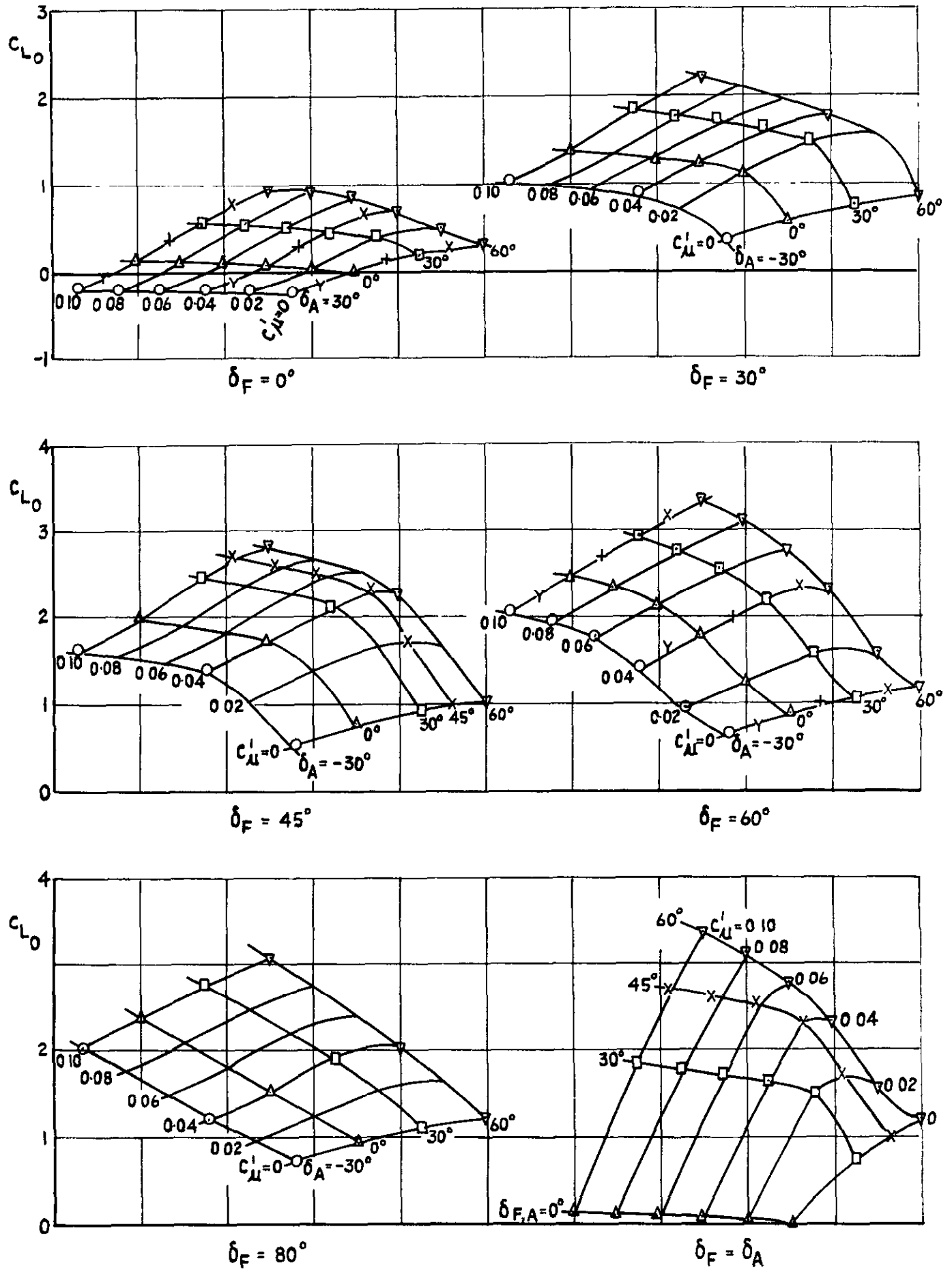

Fig. 17 Lift coefficient C_{L_0} at no lift angle for $\delta_F = \delta_A = 0°$ and $C'_\mu = 0$ ($\alpha = -3{\cdot}2°$)

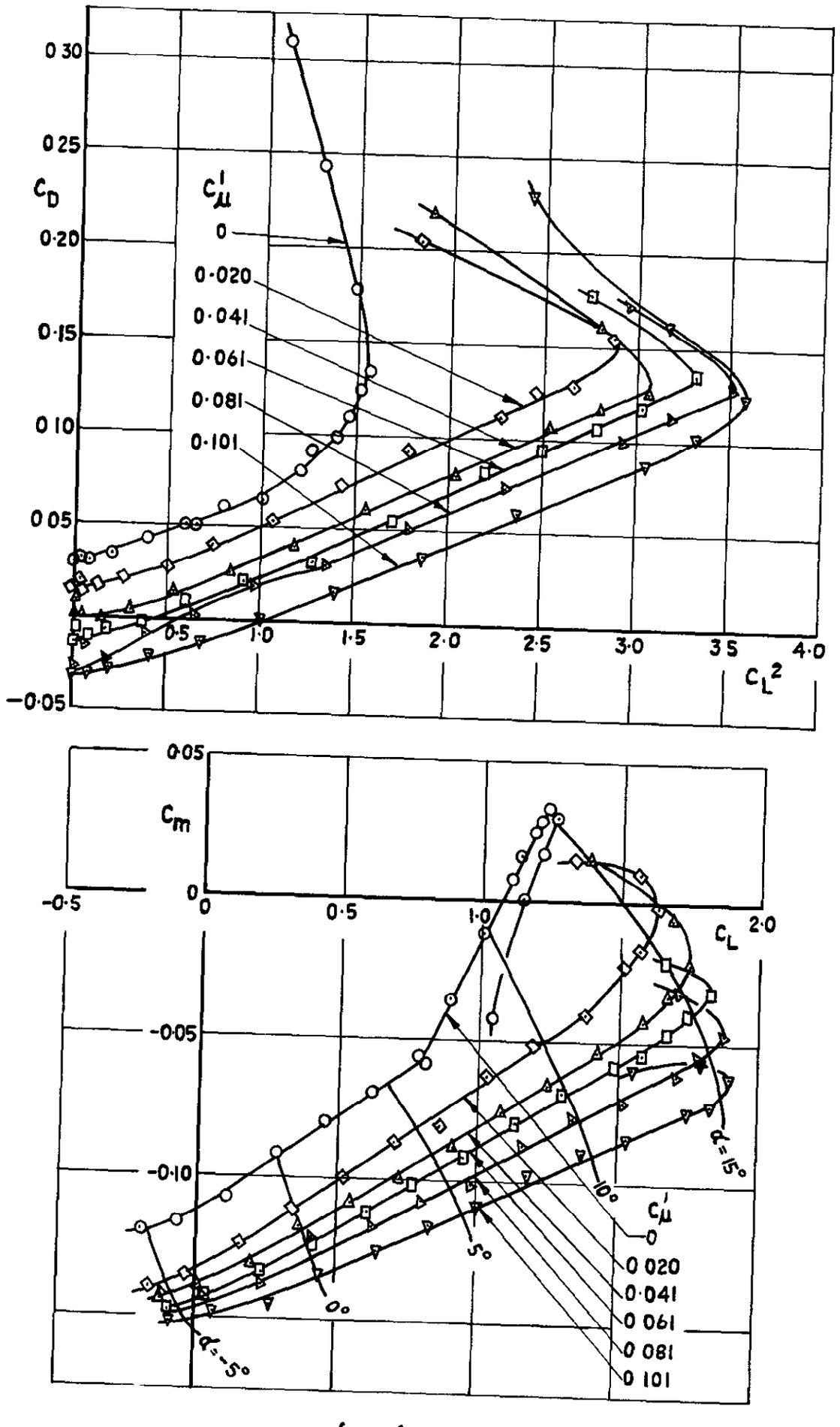

a $\delta_F = \delta_A = 0$

Fig. 18a Variation of C_D and C_m with C_L

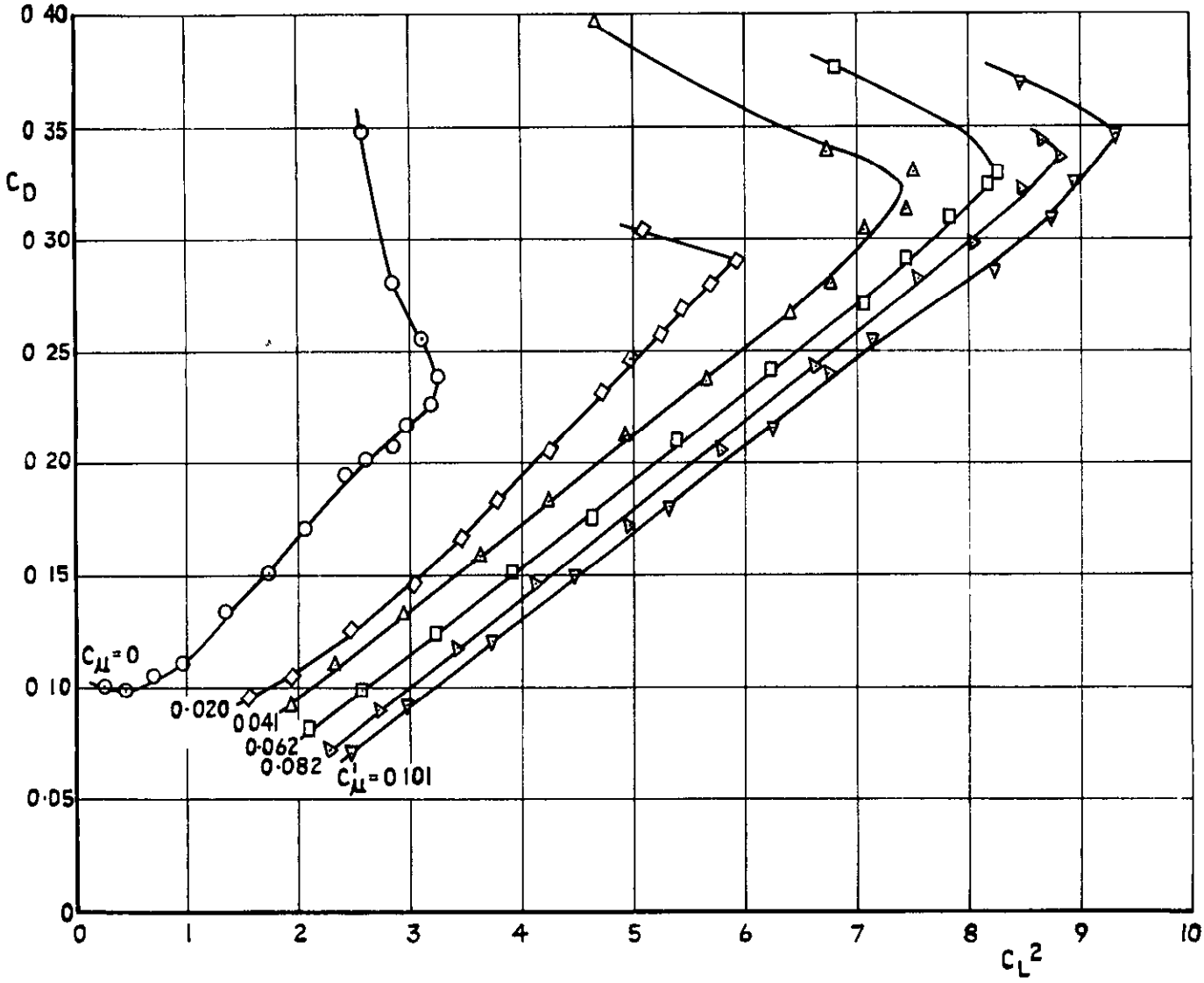

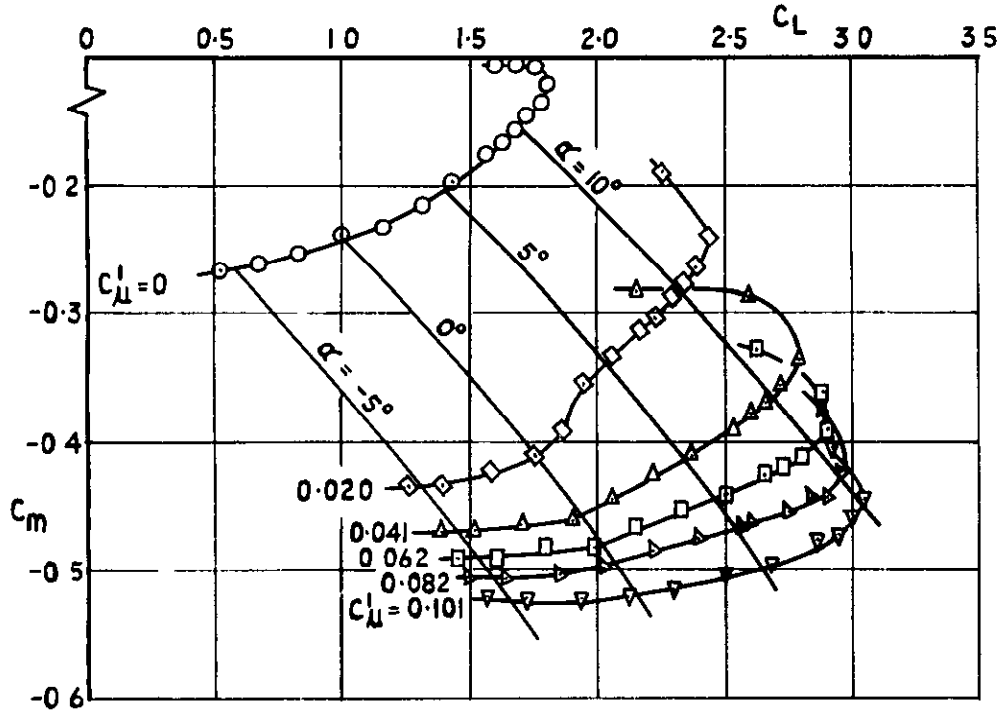

b $\delta_F = \delta_A = 30°$

Fig. 18b Variation of C_D and C_m with C_L

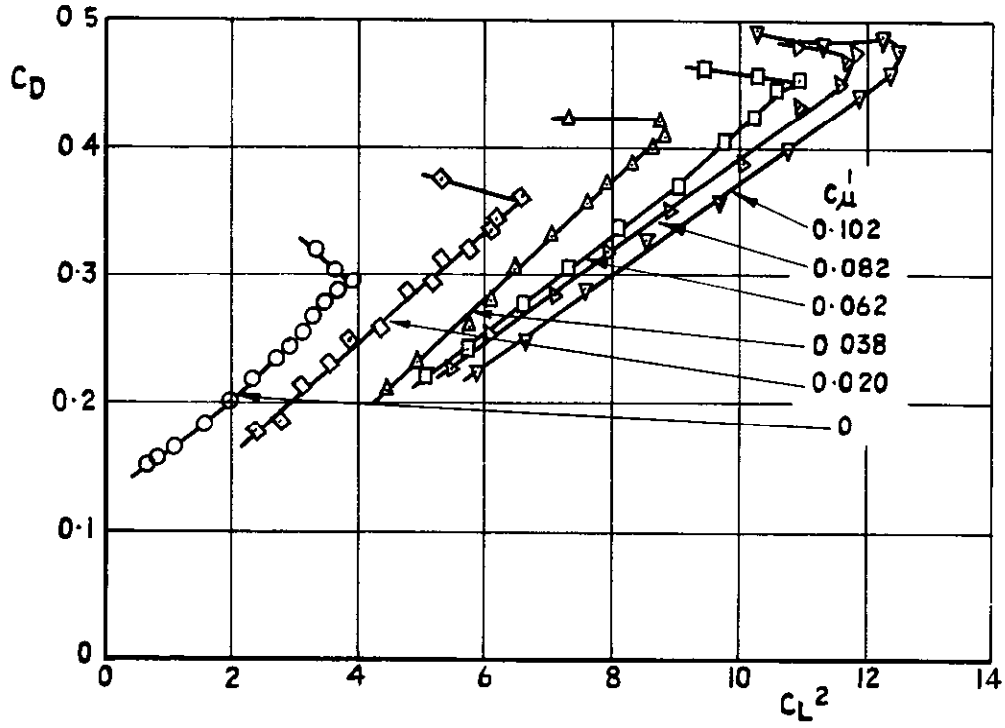

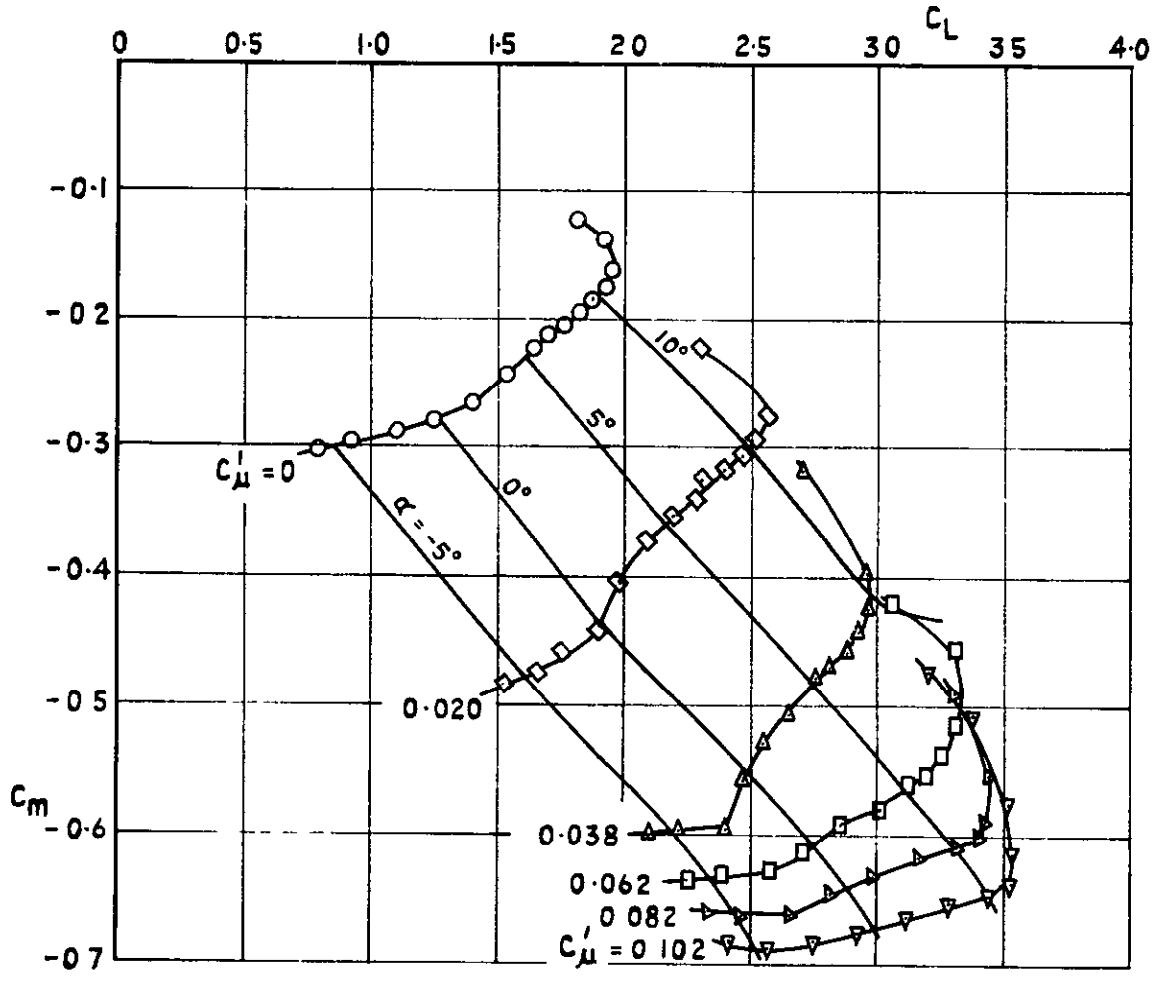

c $\delta_F = \delta_A = 45°$

Fig. 18c Variation of C_D and C_m with C_L

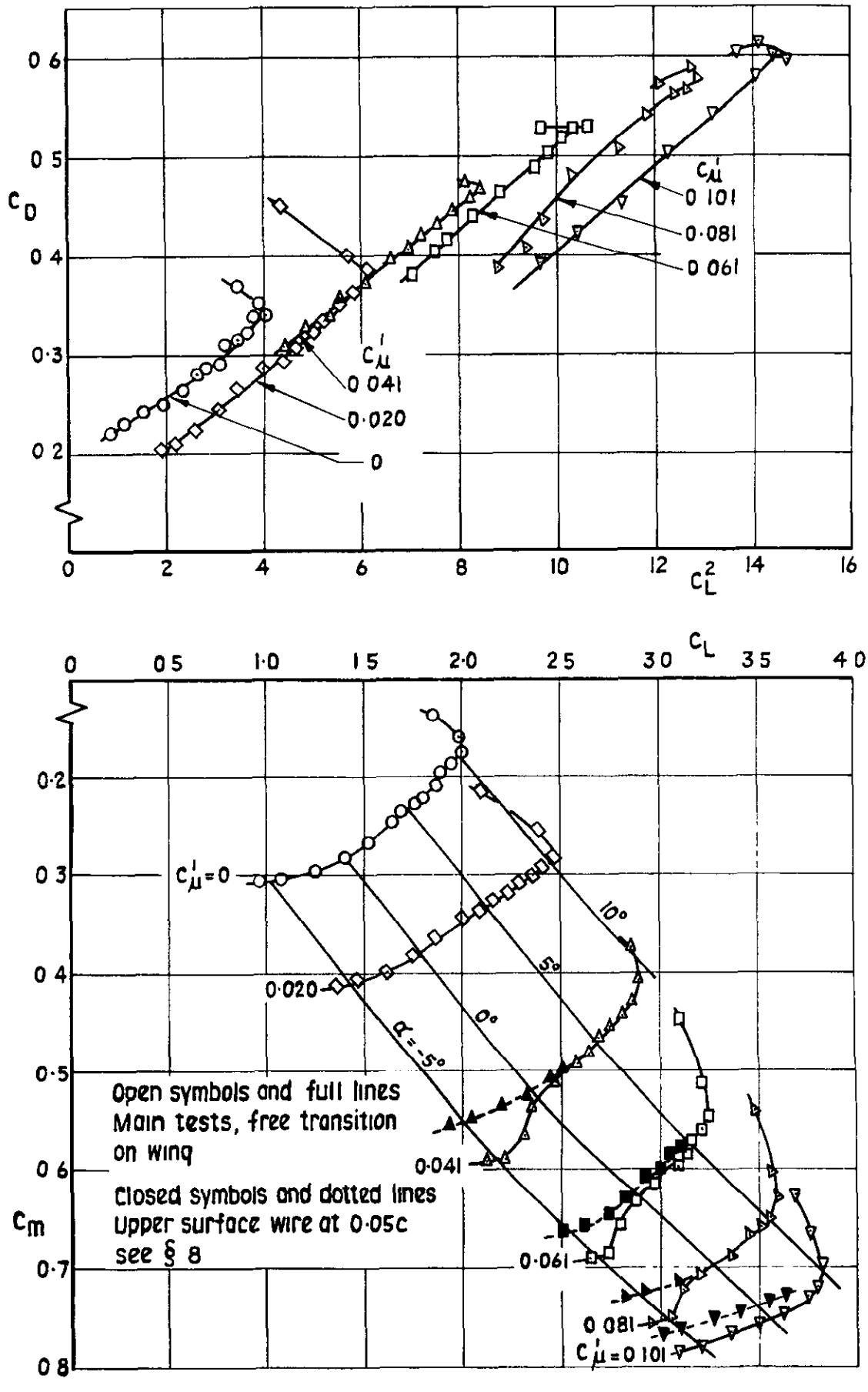

d $\delta_F = \delta_A = 60°$

Fig. 18d Variation of C_D and C_m with C_L

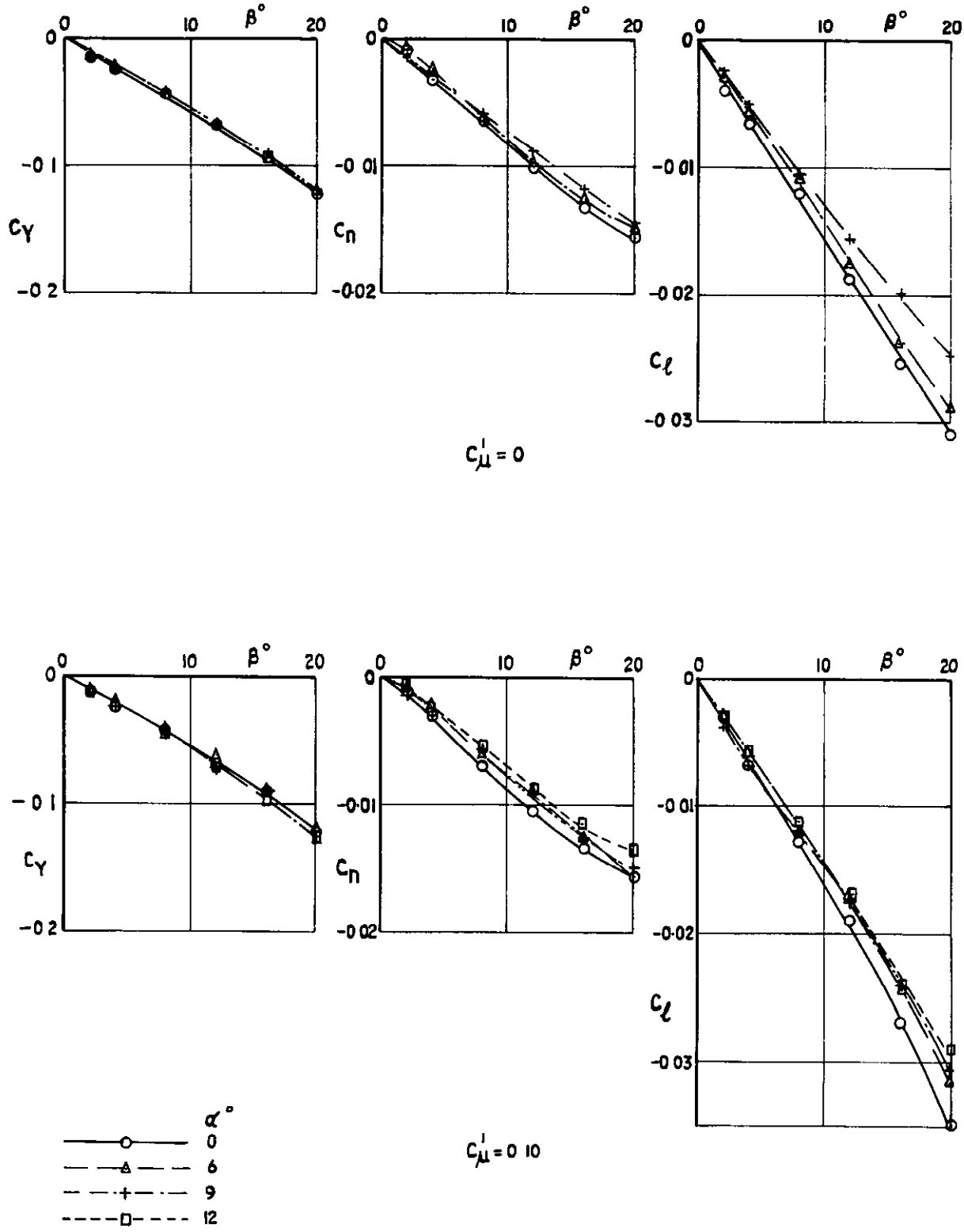

Fig.19a Lateral force and moment coefficients with sideslip
$\delta_F = \delta_A = 0°$

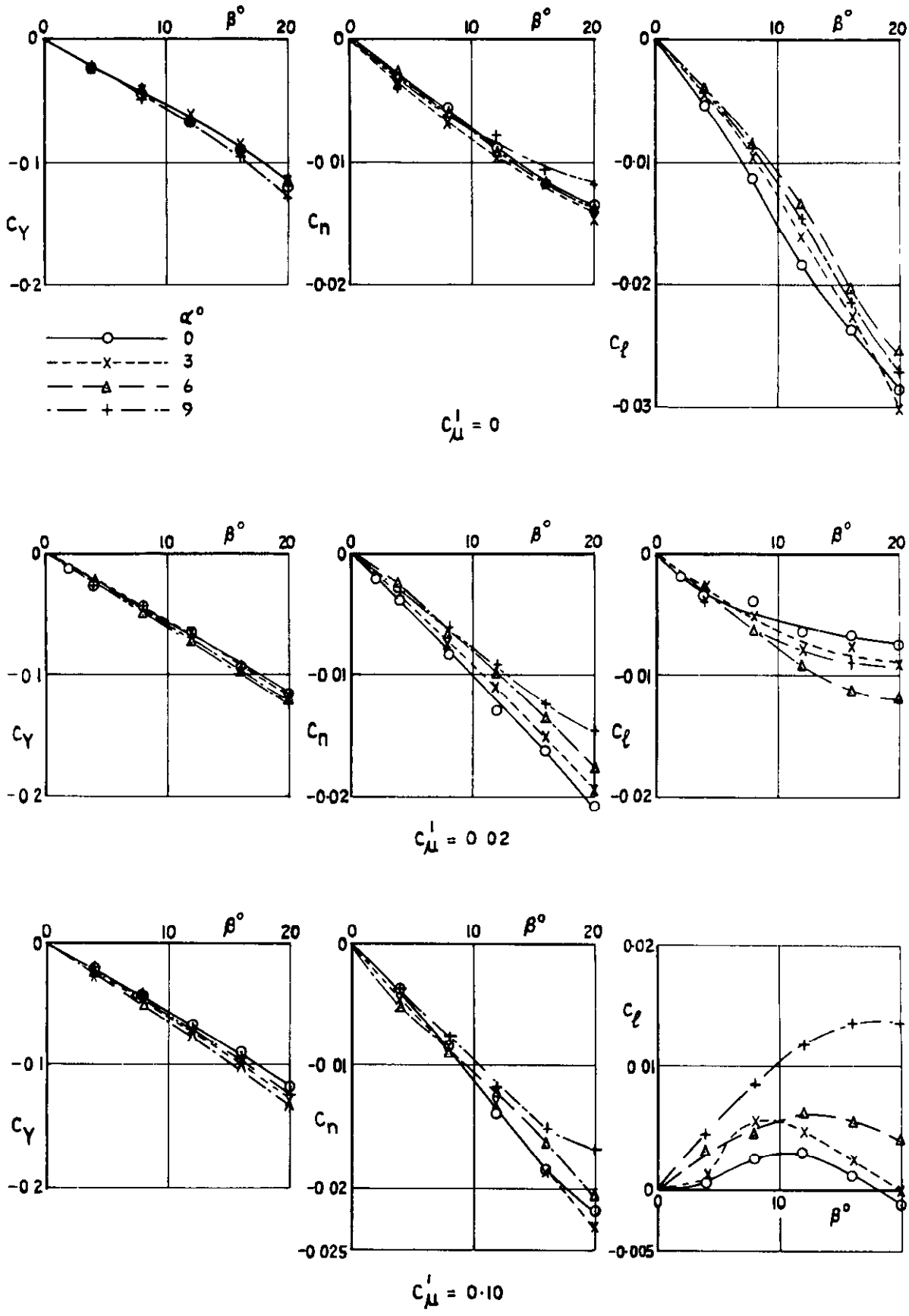

Fig. 19b Lateral force and moment coefficients with sideslip
$\delta_F = \delta_A = 30°$

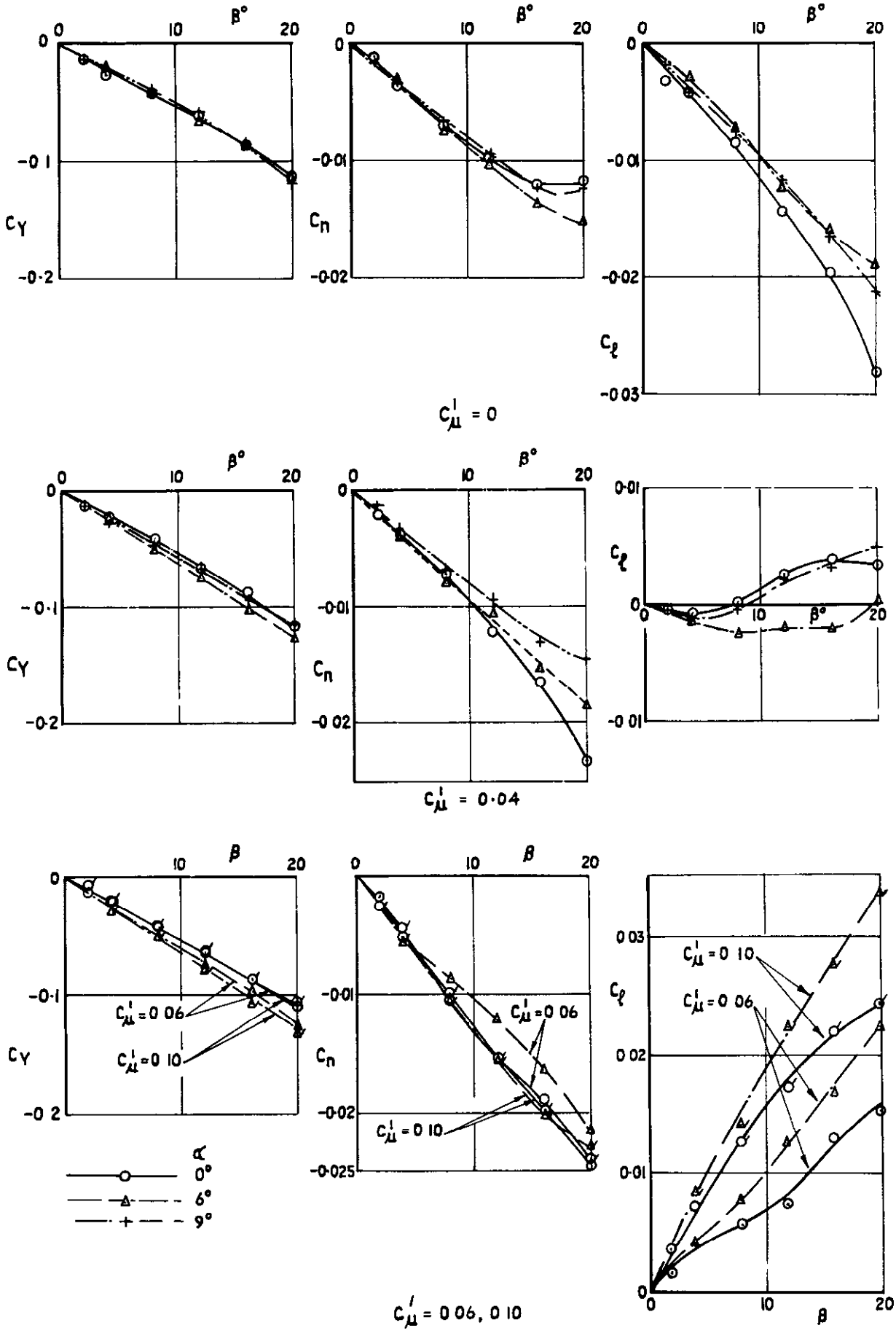

Fig. 19c Lateral force and moment coefficients with sideslip
$\delta_F = \delta_A = 45°$

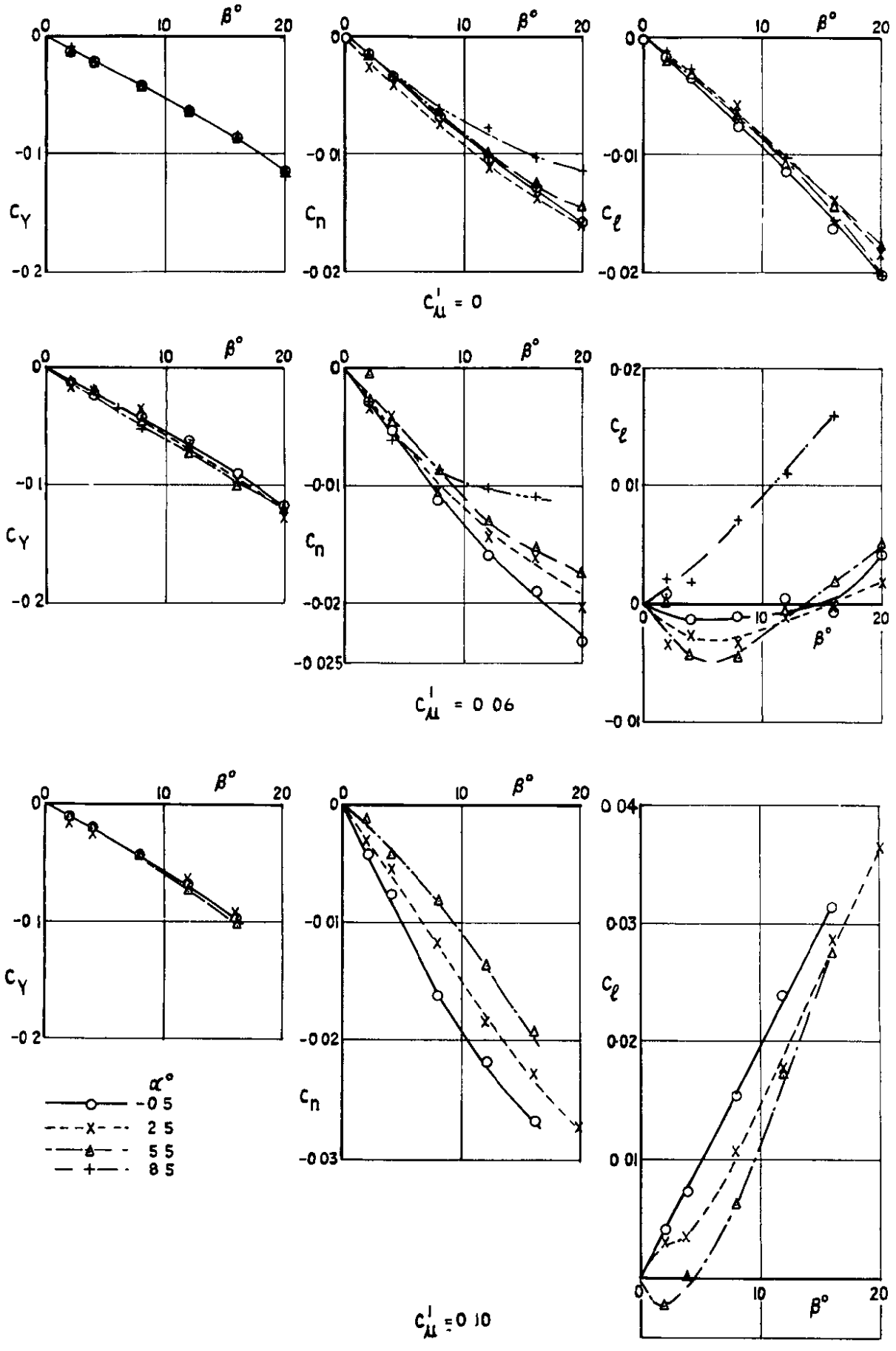

Fig. 19d Lateral force and moment coefficients with sideslip
$\delta_F = \delta_A = 60°$

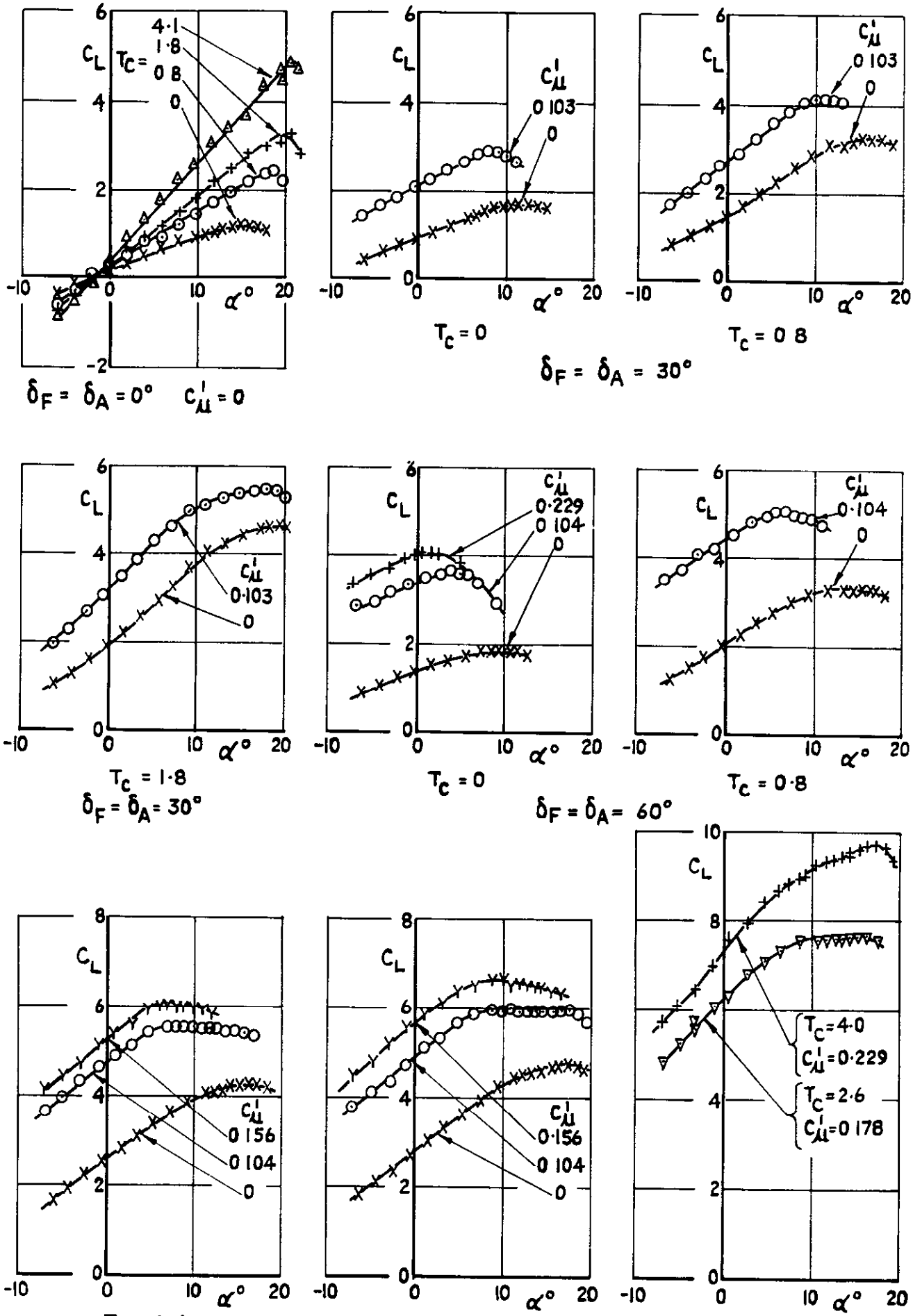

Fig 20 C_L vs α with slipstream and flap blowing

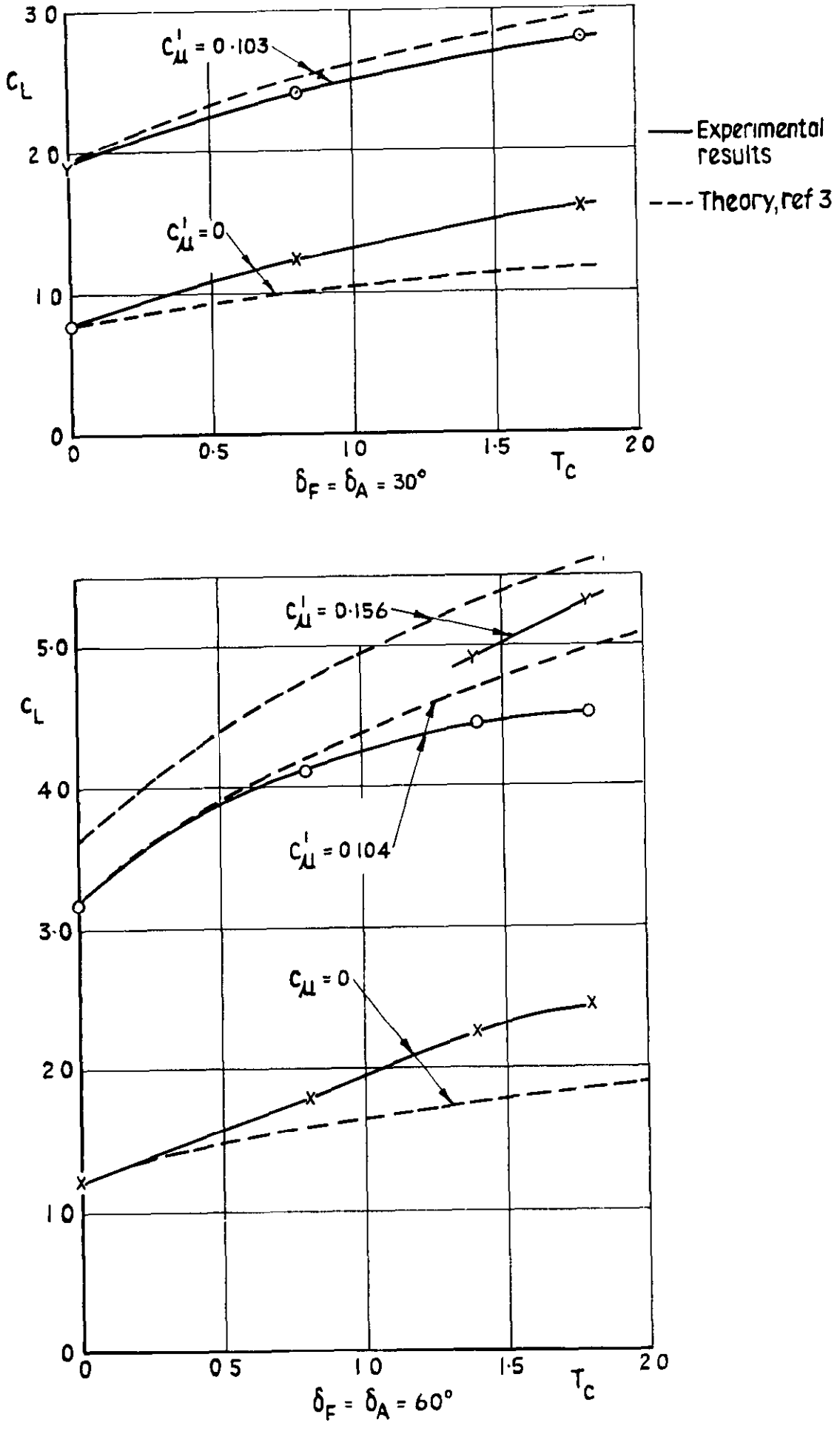

Fig 21 Effect of slipstream on lift coefficient

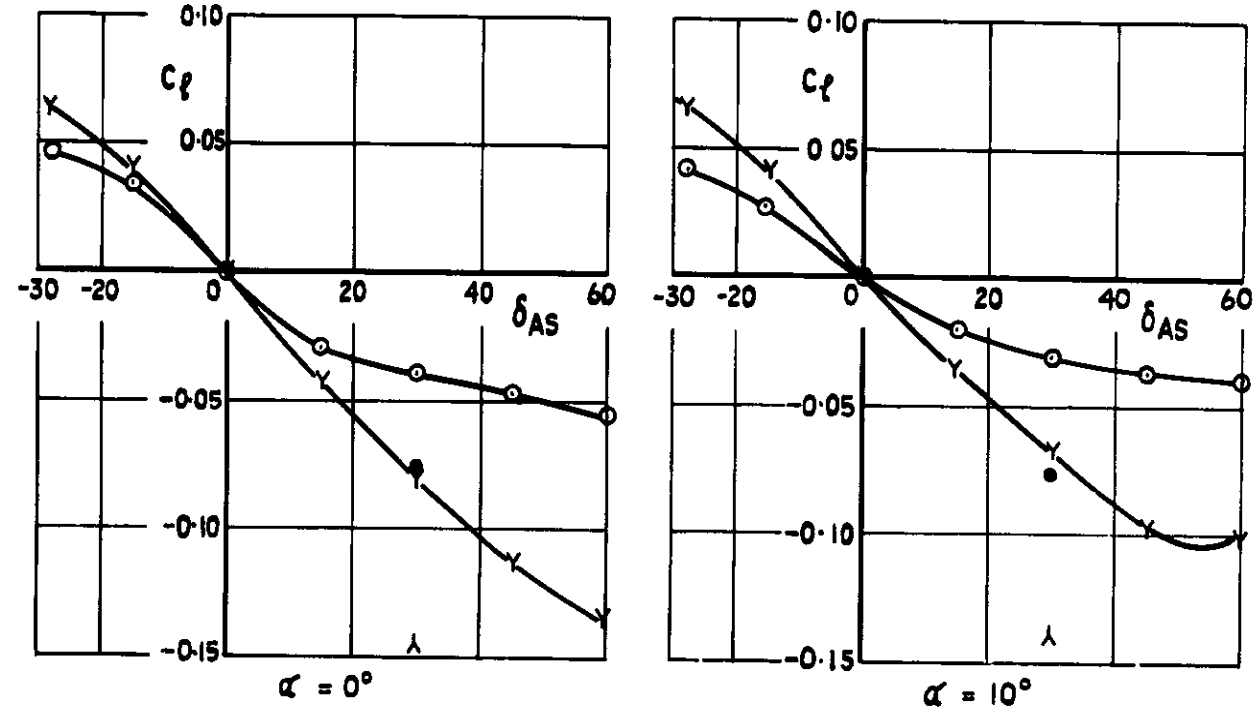

$\delta_F = 0°$

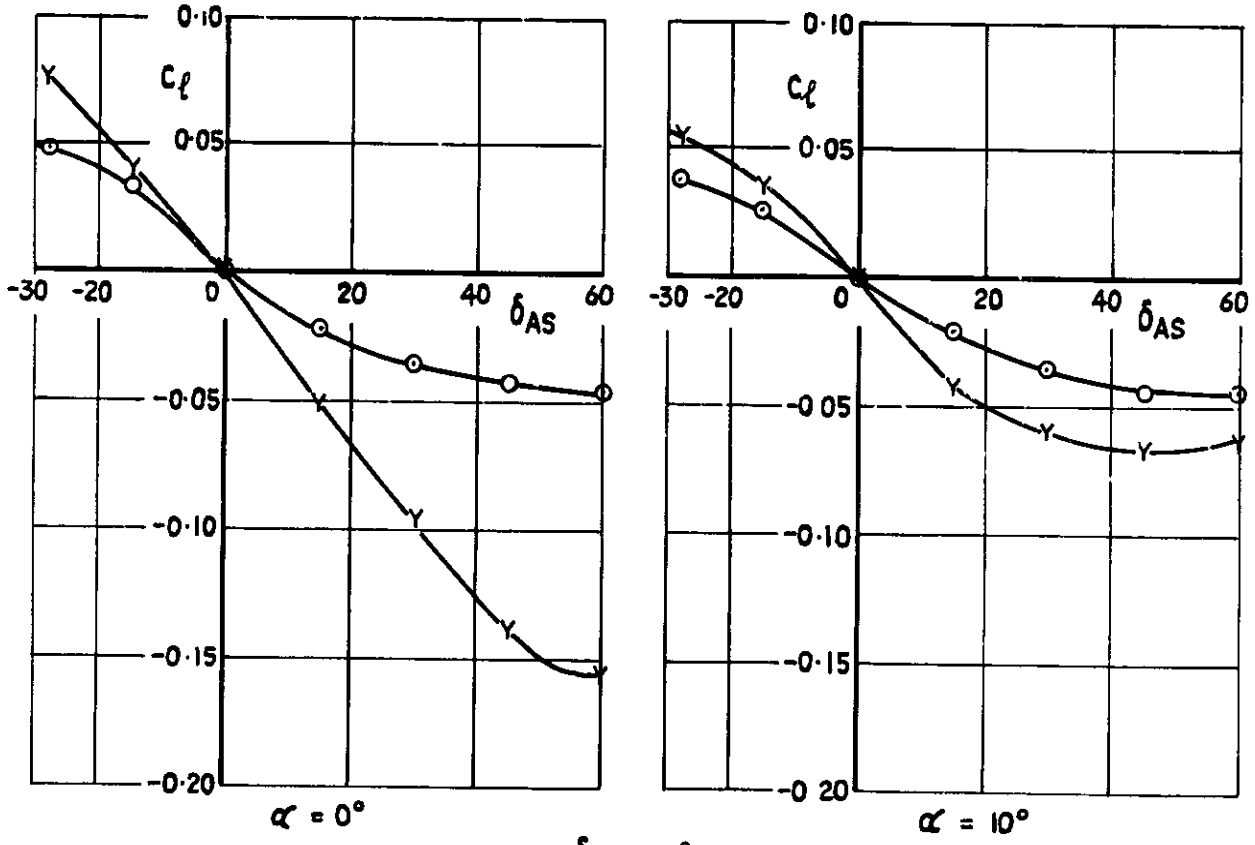

$\delta_F = 60°$

δ_{AS} = Stbd aileron angle positive downwards
δ_{AP} = Port aileron angle positive downwards

	$C'_{M} = 0$	$C'_{M} = 0{\cdot}10$
$\delta_{AP} = 0°$	—○—	—Y—
$\delta_{AP} = -28°$	•	λ

Fig 22 Aileron effectiveness

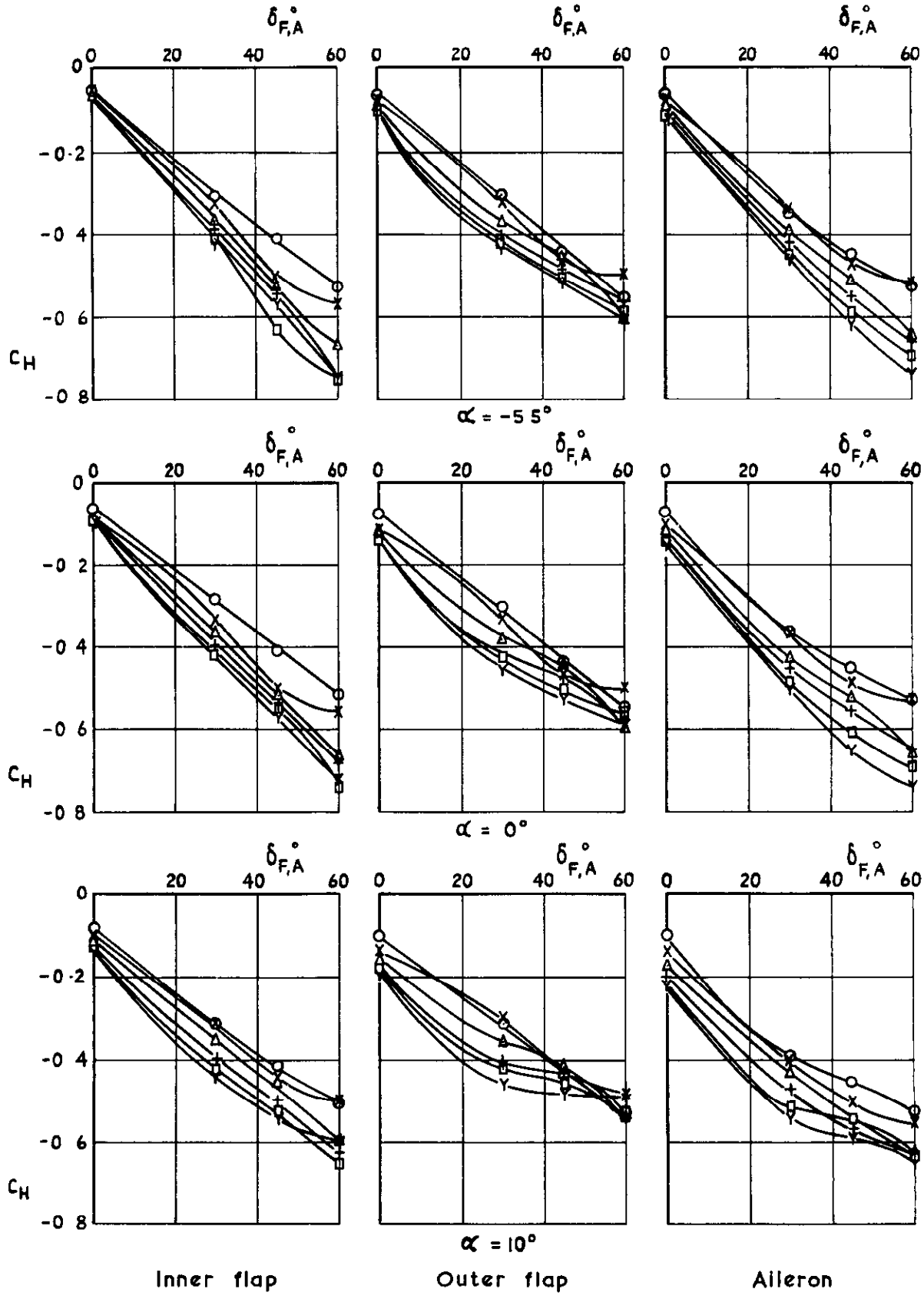

Fig.23 Control hinge moments vs control angle $\delta_F = \delta_A$ stbd wing

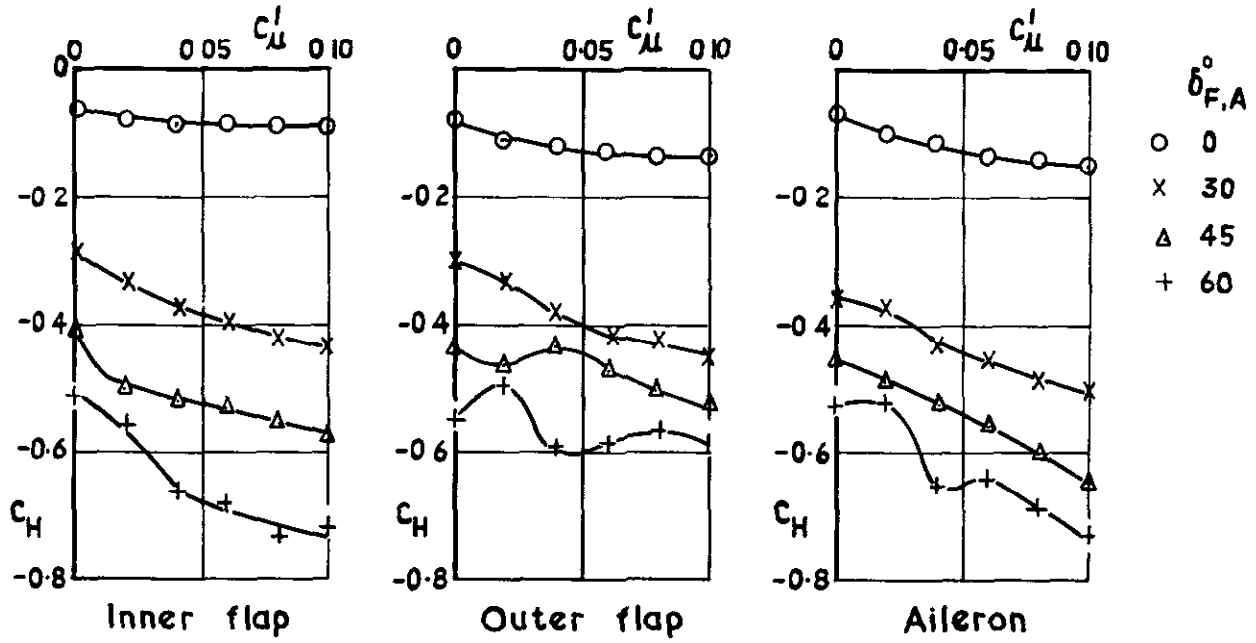

Fig 24 Control hinge moments vs C'_μ
$\delta_F = \delta_A$ Starboard wing $\alpha = 0°$

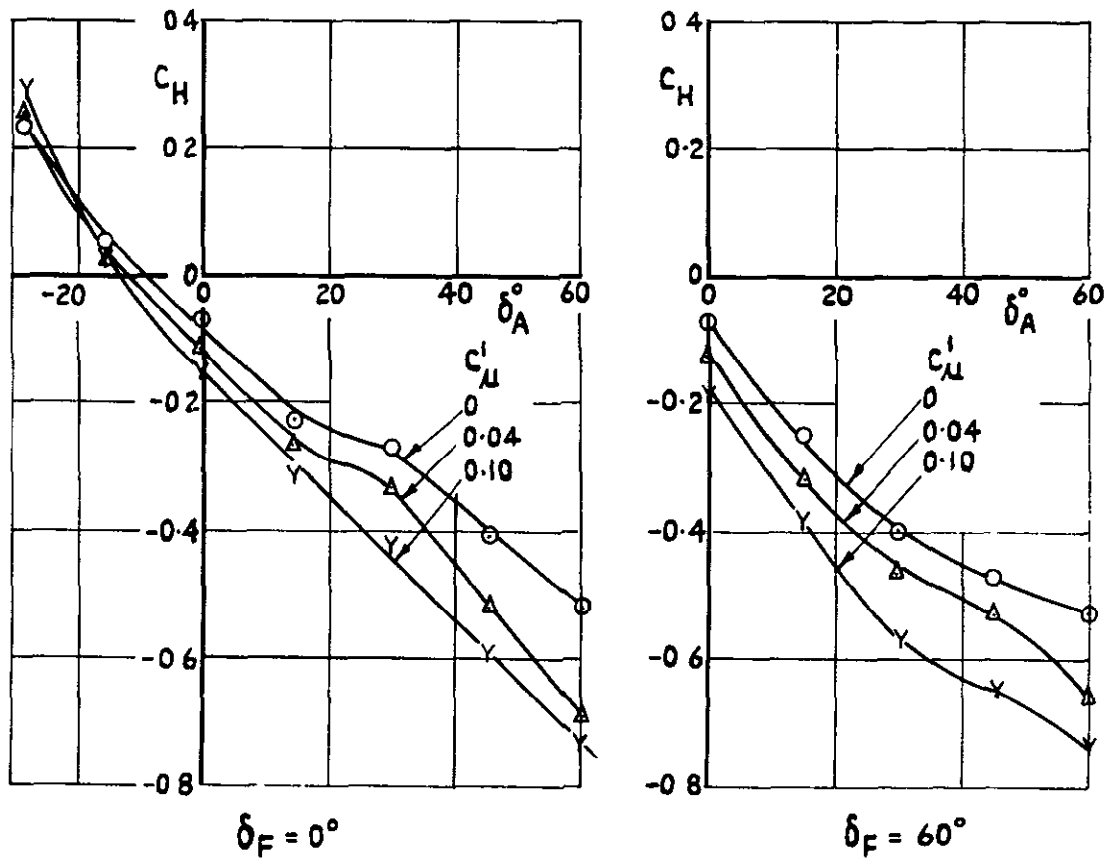

Fig 25 Aileron hinge moments $\alpha = 0°$
(Measured on starboard aileron
Both ailerons deflected in same direction positive downward)

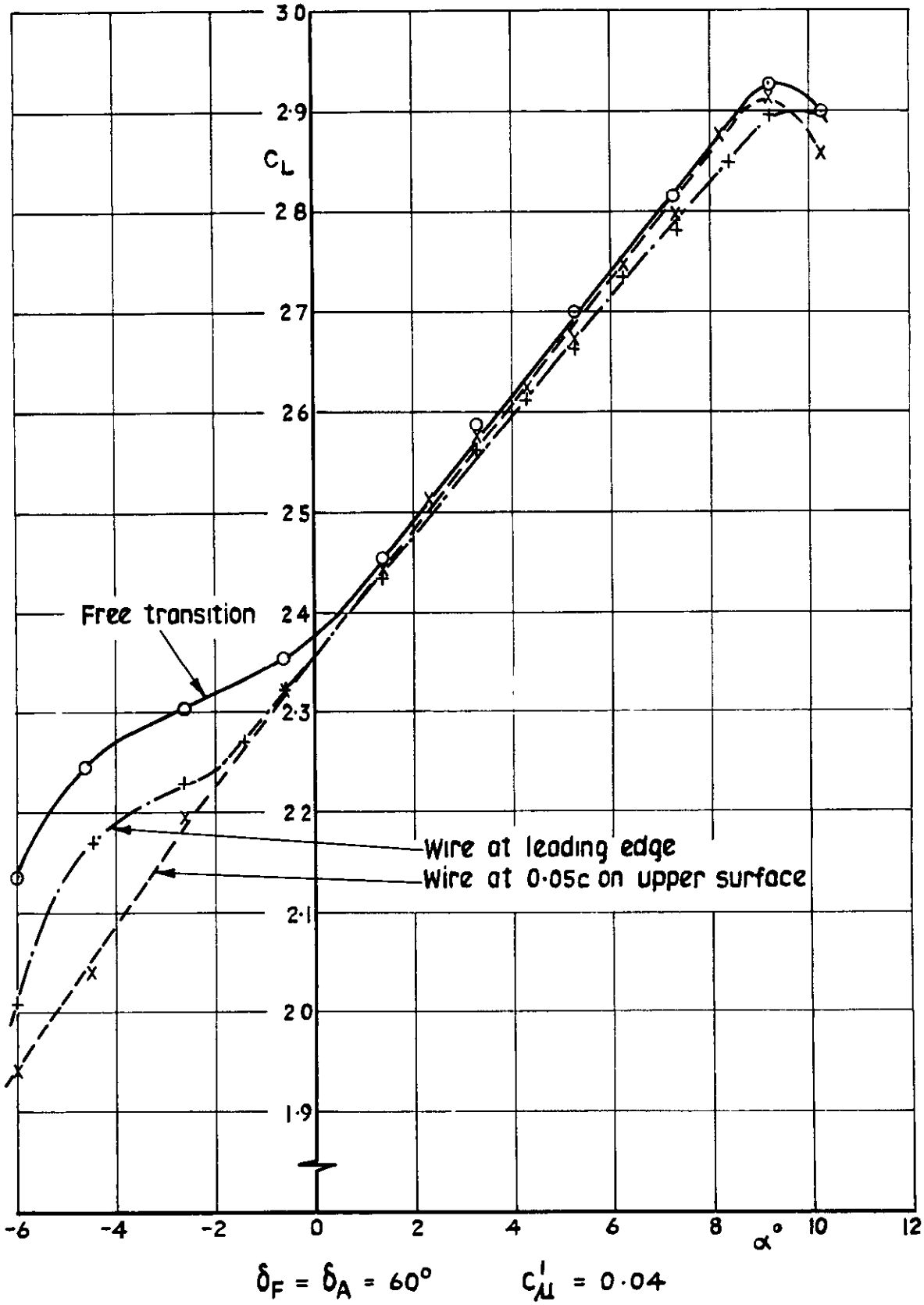

Fig 26 Non-linear effects at low incidence

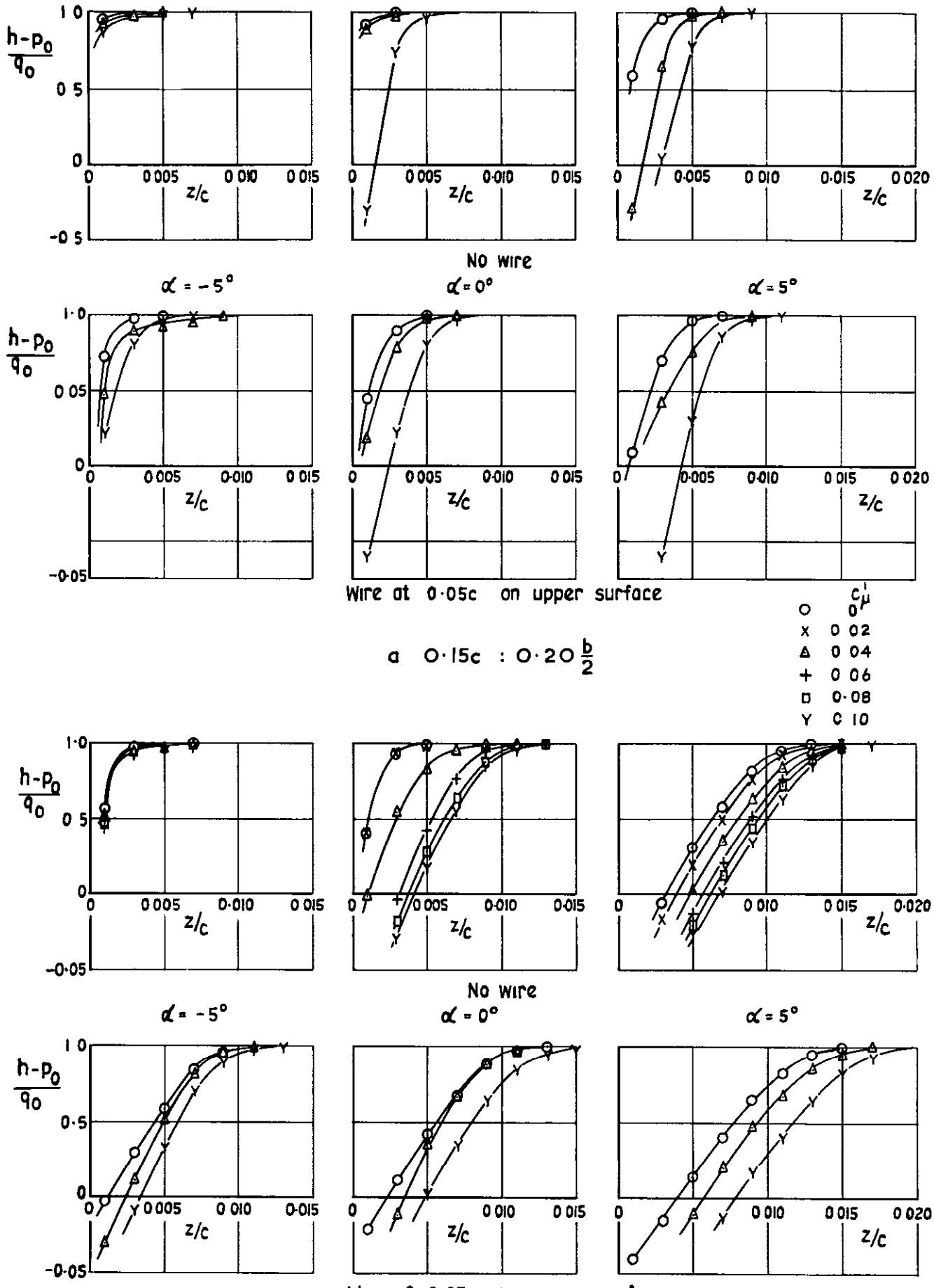

Fig.27a & b Total head in boundary layer $\delta_F = \delta_A = 60°$

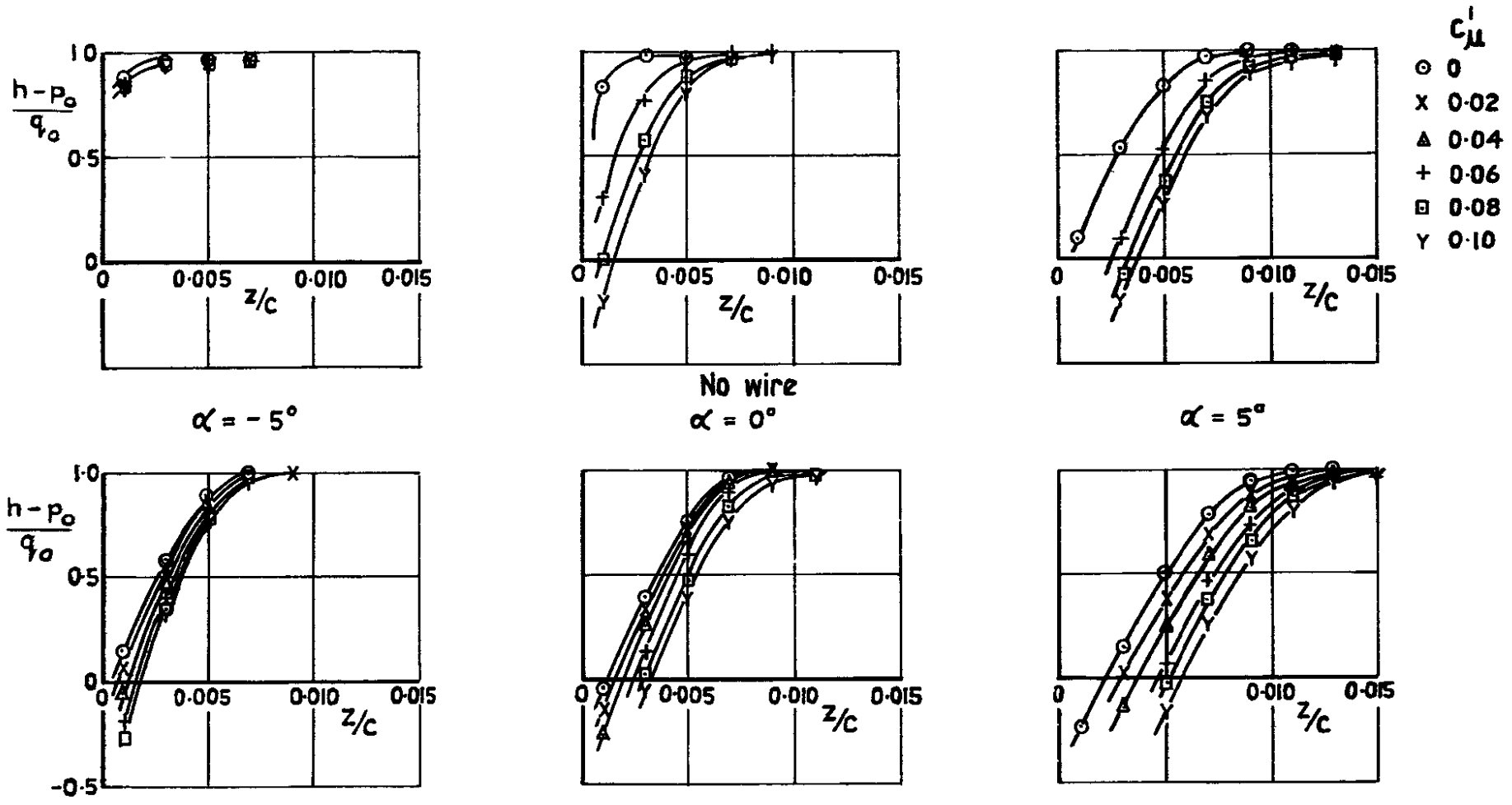

c 0·51c : 0·85 $\frac{b}{2}$

Fig. 27c Total head in boundary layer $\delta_F = \delta_A = 60°$

Printed in England for Her Majesty's Stationery Office by the Royal Aircraft Establishment, Farnborough. Dd.501371. K.5.

DETACHABLE ABSTRACT CARD

A R C C P No 1108
May 1968

Lawford, J A

533 693 2
533 6 072
533 694 511
533 695 8
533 6 071
533 6 011 32/34

LOW-SPEED WIND-TUNNEL TESTS ON AN UNSWEPT WING-FUSELAGE MODEL OF ASPECT RATIO 9 8, WITH TANGENTIAL BLOWING OVER TRAILING-EDGE FLAPS AND AILERONS, INCLUDING THE EFFECT OF SLIPSTREAM

Tests have been made on an unswept, high-wing wing-fuselage model of aspect ratio 9 8, with boundary layer control by blowing at the shroud of trailing-edge flaps and ailerons Propeller slipstream was represented during some of the tests

Critical blowing momentum coefficients were determined, these ranged from 0 015 to 0 05 at flap angles of 30° and 60° respectively With slipstream, a critical coefficient defined in terms of slipstream velocity at the propeller disc was substantially independent of thrust coefficient

(Over)

A R C C P No 1108
May 1968

Lawford, J A

533 693 2
533 6 072
533 694 511
533 695 8
533 6 071
533 6 011 32/34

LOW-SPEED WIND-TUNNEL TESTS ON AN UNSWEPT WING-FUSELAGE MODEL OF ASPECT RATIO 9 8, WITH TANGENTIAL BLOWING OVER TRAILING-EDGE FLAPS AND AILERONS, INCLUDING THE EFFECT OF SLIPSTREAM

Tests have been made on an unswept, high-wing wing-fuselage model of aspect ratio 9 8, with boundary layer control by blowing at the shroud of trailing-edge flaps and ailerons Propeller slipstream was represented during some of the tests

Critical blowing momentum coefficients were determined; these ranged from 0 015 to 0 05 at flap angles of 30° and 60° respectively With slipstream, a critical coefficient defined in terms of slipstream velocity at the propeller disc was substantially independent of thrust coefficient

(Over)

Increments of lift coefficient, without slipstream, due to a blowing momentum coefficient of 0 1, were 0 65 and 1 82 respectively at flap angles of 0^{o} and 60^{o}

Increments of lift coefficient, without slipstream, due to a blowing momentum coefficient of 0 1, were 0 65 and 1 82 respectively at flap angles of 0^{o} and 60^{o}

Published by
HER MAJESTY'S STATIONERY OFFICE

To be purchased from
49 High Holborn, London W C 1
13a Castle Street, Edinburgh EH 2 3AR
109 St Mary Street, Cardiff CF1 1JW
Brazennose Street, Manchester 2
50 Fairfax Street, Bristol BS1 3DE
258 Broad Street, Birmingham 1
7 Linenhall Street, Belfast BT2 8AY
or through any bookseller

C.P. No. 1108

SBN 11 470348 5